INSPIRe

D4.1 – Technical Report of Developments and Test of DFMC GNSS and DR VAIM

Prepared for:

Prepared by:	GMV INSPIRe TEAM GRAD INSPIRE TEAM
Contributions by:	GRAD INSPIRE TEAM
Approved by:	M Pattinson (GMV)
Authorized by:	T Richardson (GMV)
Code:	INSPIRe-GMVNSL-D4.1-v1.1
Version:	1.1
Date:	January 2024

Change Record

Issue / Rev	Date	Change Record	Authors
v1.0	13/11/2023	The first version of the deliverable submitted ESA	GMV INSPIRe Team
v1.1	18/01/2024	This version is updated based on ESA's RIDs received on December 8, 2023. Major changes are reflected in Section 6.1. Additionally, the results have been revised to showcase the DFMC VAIM-enabled findings, eliminating the need for references to GPS L1 results.	GMV INSPIRe Team

TABLE OF CONTENTS

List of Tables and Figures

1 INTRODUCTION

1.1 Purpose

This deliverable document is one of the main outputs of WP4 of the INSPIRe project, titled D4.1: Technical Report on the Development and Testing of DFMC GNSS and Dead Reckoning (DR) VAIM. The task within WP4 has explored, developed, and tested techniques and algorithms for the integration of dual frequency, multiconstellation GNSS and dead reckoning to create a vessel autonomous integrity monitoring (VAIM) solution, similar to the well-established aircraft autonomous integrity monitoring (AAIM) concept used in aviation. This should further enhance user-level integrity and provide additional resilience in the navigation solution.

The purpose of this report is to document the activities that have been completed, including:

- Generate a clear concept definition for VAIM.
- Assess and trade-off different GNSS and dead reckoning loose coupling schemes to Identify the best approach for the maritime environment and requirements, considering the Likely future requirement to extend the solution to other inputs from the resilient PNT system-of-systems.
- Define VAIM algorithms based on the preferred loose coupling scheme.
- Define an outline functional design for the VAIM solution comprising dual frequency, multiconstellation GNSS and dead reckoning within a test environment.
- Prototype the algorithms using a suitable software application (such as MATLAB).
- Test and evaluate the prototype algorithms within a test environment using simulated and/or real data, to verify the outline functional design.
- Assess the feasibility of a maritime VAIM solution (considering not only technical issues but also affordability).

1.2 Scope

Following the introduction to the document presented in Section 1, the layout of the remainder of the document is as follows:

- **Section 2** contains a list of applicable and reference documents
- **Section 3** presents the concept definition of VAIM
- **Section 4** describes the high-level algorithm design
- **Section 5** presents the description of the algorithm testing
- **Section 6** provides the evaluation of the algorithm
- **Section 7** provides a feasibility assessment of the VAIM algorithm

1.3 Definitions and Acronyms

1.3.1 Definitions

Concepts and terms used in this document and need defining are included in the following table:

Table 1-1 Definitions

Concept / Term	Definition
M(G)RAIM	Maritime General-RAIM: is a chi-squared fault-detection process with simple geometric screening rules to ensure safety
MRAIM	Maritime RAIM: is a maritime-specific implementation of the aviation ARAIM concept and performs a multiple-hypothesis solution-separation process, then computes a protection level and iteratively optimises this PL through re-allocation of integrity risk
VAIM	Vessel Autonomous Integrity Monitoring: this is a maritime-specific implementation of the M(G)RAIM concepts developed in this project to provide the requested integrity including dead-reckoning techniques, similar to aircraft autonomous integrity monitoring (AAIM) concept used in aviation, enhancing user-level integrity and providing additional resilience in the navigation solution

1.3.2 Acronyms

Acronyms used in this document and need defining are included in the following table:

Table 1-2 Acronyms

Acronym	Definition
AL	Alert Limits
ARAIM	Advanced Receiver Autonomous Integrity Monitoring
CDF	Cumulative distribution function
DFMC	Dual Frequency Multiconstellation
DGNSS	Differential GNSS
DGPS	Differential GPS
DOP	Dilution of Precision
DR	Dead Reckoning
ECAC	European Civil Aviation Conference
EGNOS	European Geostationary Navigation Overlay Service
EKF	Extended Kalman Filter
ESA	European Space Agency
FD	Fault Detection
FDE	Fault Detection and Exclusion
GBAS	Ground-Based Augmentation System
GEAS	GNSS Evolutionary Architecture Study
GLONASS	GLObal NAvigation Satellite System
GNSS	Global Navigation Satellite System
GPS	Global Positioning System
GRAD	GLA Research and Development
GSA	European GNSS Agency
HAL	Horizontal alarm Limit
HDOP	Horizontal Dilution of Precision
HMI	Hazardous Misleading Information
HPE	Horizontal Position Error
HPL	Horizontal Protection Level
HUL	Horizontal Uncertainty Level
IALA	International Association of Marine Aids to Navigation and Lighthouse Authorities
ICAO	International Civil Aviation Organisation
IEC	International Electrotechnical Commission
INSPIRe	Integrated Navigation System-of-Systems PNT Integrity for Resilience
IMO	International Maritime Organisation
IR	Integrity Risk
ISM	Integrity Support Message
LPV	Localizer Performance with Vertical guidance
MHSS	Multiple Hypothesis Solution Separation
MOPS	Minimum Operational Performance Standards
MGRAIM	Maritime General RAIM
MRAIM	Maritime RAIM
MSC	Maritime Safety Committee
MSI	Maritime Safety Information
MSR	Multi-system shipborne receiver
N/A	Not Applicable
NLOS	Non-Line of sight
NPA	Non-Precision Approach
PFA	Probability of False Alarm
PL	Protection Level
PHMI	Probability of Hazardously Misleading Information
PMD	Probability of Miss detection

PNT	Positioning Navigation and Timing
PVT	Position, Velocity and Time
RAIM	Receiver Autonomous Integrity Monitoring
RTCA	Radio Technical Commission for Aeronautics
RTK	Real-time kinematic positioning
SARPS	Standards and Recommended Practices
SBAS	Satellite Based Augmentation System
SIS	Signal in Space
SOLAS	Safety at Life at Sea
TBC	To Be Confirmed
TTA	Time to Arrival
UL	Uncertainty Level
VAL	Vertical alarm Limit
VAIM	Vessel Autonomous Integrity Monitoring
VHF	Very High Frequency

2 REFERENCES

2.1 Applicable Documents

The following documents, of the exact issue shown, form part of this document to the extent specified herein. Applicable documents are those referenced in the Contract or approved by the Approval Authority. They are referenced in this document in the form [AD.x]:

Table 2-1 Applicable Documents

Ref.	Title	Code	Version	Date
[AD.1]	INSPIRe Technical Proposal, Taylor Airey	T-062-001-02 Part 1	-	June 2022
[AD.2]	INSPIRe Management Proposal, Taylor Airey	T-062-001-02 Part 2	-	June 2022
[AD.3]	INSPIRe Proposal GMV	GMV 10842/21	V2/21	

2.2 Reference Documents

Although not part of this document, the following documents amplify or clarify its contents. Reference documents are those not applicable and referenced within this document. They are referenced in this document in the form [RD.x]:

Table 2-2 Reference Documents

Ref.	Title	Code	Version	Date
[RD.1]	A.915(22) Revised Maritime Policy and Requirements for a Future Global Navigation Satellite System (GNSS)	IMO/A.915 (22)	-	29/11/2001
[RD.2]	A.1046(27) Service Requirements for Worldwide Radio Navigation Systems	IMO/A.1046(27)	-	30/11/2011
[RD.3]	MSC.401(95) Performance Standards for Multi-System Shipborne Radionavigation Receivers	IMO/MSC.401(95)	-	8/06/2015
[RD.4]	MSC.1/Circular.1575 - Guidelines for Shipborne Position, Navigation and Timing (PNT) Data Processing – (16 June 2017)	MSC.1/Circular.1575	-	06/2017
[RD.5]	Resolution MSC.112(73) - Adoption of the Revised Performance Standards for Shipborne Global Positioning System (GPS) Receiver Equipment	MSC.112(73)	-	12/2000
[RD.6]	Resolution MSC.53(66) - Performance Standards for Shipborne GLONASS Receiver Equipment - (Adopted on 30 May 1996)	MSC.53(66)	-	05/1996
[RD.7]	Resolution MSC.233(82) Adoption of The Performance Standards for Shipborne Galileo Receiver Equipment - (Adopted On 5 December 2006)	MSC.233(82)	-	12/2006
[RD.8]	RESOLUTION MSC.114(73)) Adoption of The Revised Performance Standards for Shipborne DGPS And DGLONASS Maritime Radio Beacon Receiver Equipment. (Adopted on 1 December 2000	MSC 73/21/Add.3	-	12/2000
[RD.9]	INSPIRe D2.1 – Technical Report of Developments and Test of GPS M(G)RAIM	INSPIRe-GMV-D2.1	V1.3	02/2023
[RD.10]	INSPIRe D3.1 – Technical Report of Developments and Test of DFMC M(G)RAIM	INSPIRe-GMV-D3.1-	V1.2	05/2023
[RD.11]	S. F. Appleyard, “Marine Electronic Navigation”, Feb 1988, ISBN 0-7102-1271-2.	-	-	02/1998
[RD.12]	Vectornav Inertial System webpage	-	-	05/2023

	https://www.vectornav.com/resources/inertial-navigation-articles/what-is-an-ins			
[RD.13]	INSPIRe – 400013852522NLRR –WP4 Alg4.1 - Algorithm documentation DFMC & DR VAIM - v1.0	INSPIRe-GMVNSL-Alg4.1-v1.0	V1.0	11/2023
[RD.14]	Lee, Jinsil, Kim, Minchan, Lee, Jiyun, Pullen, Sam, "Integrity assurance of Kalman-filter based GNSS/IMU integrated systems against IMU faults for UAV applications," *Proceedings of the 31st International Technical Meeting of the Satellite Division of The Institute of Navigation (ION GNSS+ 2018)*, Miami, Florida, September 2018, pp. 2484-2500. https://doi.org/10.33012/2018.15977	N/A	N/A	09/2018
[RD.15]	INSPIRe - 400013852522NLRR –WP4 Spec4.1 – Functional Test Specification DFMC & DR VAIM-v1.0	INSPIRe-GMVNSL-Spec4.1-v1.0	V1.0	11/2023
[RD.16]	INSPIRe - 400013852522NLRR –WP4 Spec4.1 – Functional Test Specification DFMC & DR VAIM-v1.0 -TEST REPORT-v1.0	INSPIRe-GMVNSL-Spec4.1(Test Report)-v1.0	V1.0	11/2023

3 CONCEPT DEFINITION FOR VAIM

3.1 Introduction

This section provides a clear definition of VAIM based on the integration of dual frequency, multiconstellation GNSS and dead reckoning, which can be expanded to include other inputs in the future.

The term "dead reckoning" refers to the estimation of a current position using a previously known position and measurements of distance (or integrated velocity) and direction travelled. The speed is typically measured in body-aligned axes, so attitude (at least heading) is required to obtain the direction of travel relative to a local reference frame.

M(G)RAIM is developed for the GNSS positioning technique, which is only one of the multiple sensors available on board a vessel. The main purpose of the VAIM algorithm is to exploit the capabilities of the most common navigation sensors installed on a vessel when they are combined. There are different techniques, but the VAIM algorithm will explore loose coupling architectures to be aligned with the IMO/MSC.401(95) [RD.3] concept, in which several sensors provide positioning and integrity information to a processing unit, which provides the final positioning and integrity.

The high-level concept of this VAIM algorithm is to expand the capabilities of the M(G)RAIM algorithms detailed in [RD.10]. The idea behind VAIM is to use information from non-GNSS sensors to perform a consistency check on the positioning domain, and to perform a safe propagation technique of the last GNSS estimated epoch and its positioning accuracy of 95% (ACC95) or protection level (PL) in case of GNSS outage or significant performance degradation to improve performance.

The following chapters review the different sensors available on board, along with their typical performance and main features. Then, they will assess dead reckoning loose coupling techniques to hybridize GNSS positioning, providing the required level of integrity.

3.2 Sensor Types & Performance

This section details the main sensors placed on board. First, it identifies the different sensors available on SOLAS vessels, which will be crucial in defining the VAIM architecture. Different sensors provide different types of information, and not all integrity concepts are suitable for every sensor.

It is important to note that only SOLAS vessels are considered in this paper, as non-SOLAS vessels could employ any type of sensor, which would introduce too much complexity. Regulation 19 of the SOLAS V Safety of Navigation Convention defines navigation equipment carriage requirements based on the ship's usage and gross tonnage. A subset of navigation sensor requirements is summarized in Table 3-1. The convention allows "other means" to be used in place of these sensors.

Ship type	Navigation sensor carriage requirement
All Ships	Adjusted magnetic compass, GNSS Receiver
Over 150gt & All Passenger Ships	Spare magnetic compass
Over 300gt & All Passenger Ships	Speed and distance measuring device (through water) Echo sounding device
Over 500gt (non-international) & All Passenger Ships	Gyro compass
Over 3000gt	3 GHz Radar
Over 50000gt	Rate of turn indicator Speed and distance measuring device (over the ground in the forward and athwartships direction)

Table 3-1 SOLAS V R19 Sensor Carriage Requirements

Regulation 19 of the SOLAS V Safety of Navigation Convention states integrated bridge systems shall be so arranged that failure of one subsystem does not cause failure to any other sub-system. In case of failure in one part of an integrated navigational system, it shall be possible to operate each other individual item of equipment or part of the system separately.

This means that tight coupling schemes are risky since the failure of one sensor or subsystem could lead to complete navigation failure. That is why VAIM only considers loose coupling techniques. Taking all of this into consideration, the following potential sensor schemes will be analysed for VAIM performance:

- GNSS + Gyro/magnetic compass + Speed sensor
- GNSS + IMU

3.2.1 Compasses

A magnetic compass is an instrument for determining direction on the surface of Earth by means of a magnetic pointer that aligns itself with Earth's magnetic field.

A magnetic compass works because the Earth acts as a magnetic dipole, generating a huge magnetic field. The Earth has two magnetic poles near the North and South poles. This magnetic field of the Earth causes a magnetized needle of iron or steel to swing freely into a north-south position.

However, compasses give the direction of magnetic north, which is not always the same as true/geographic north, which is a fixed point on the globe. Magnetic north is aligned with the Earth's magnetic field, and it shifts and changes over time in response to changes in the Earth's magnetic core. The difference between magnetic and geographic north is called magnetic declination and may be different for each Earth location.

Another type of compass is a gyrocompass, which is a non-magnetic compass based on a fast-spinning disc and the rotation of the Earth to find geographic direction automatically. A gyroscope is an essential component of a gyrocompass, but they are different devices. A gyrocompass is built to use the effect of gyroscopic precession, which is a distinctive aspect of the general gyroscopic effect.

Gyrocompasses are widely used for navigation on ships because they have two significant advantages over magnetic compasses:

- they find true north as determined by the axis of the Earth's rotation, which is different from, and navigationally more useful than, magnetic north, and
- they are unaffected by ferromagnetic materials, such as in a ship's steel hull, which distort the magnetic field.

3.2.2 Speed Sensors

There are several kinds of speed sensors used for boats. First for all, A traditional boat speedometer uses a pitot tube to measure the speed of the water passing by the boat. The pitot tube is a long, thin tube that is open at one end and has a small hole in the other end. The pitot tube is placed in the water so that the open end is facing the direction of the water flow. As the water flows past the pitot tube, it creates a pressure difference between the inside and outside of the tube. This pressure difference is proportional to the speed of the water relative to the vessel. This is not a direct indication of the vessel speed relative to ground, since the water is moved by current and waves.

The second type, which does not use GNSS technology, is a boat electric paddle wheel. This is a device that consists of a paddle wheel attached to the back of the boat and a sensor mounted on the front of the boat. The paddle wheel spins as the boat moves through the water, and the sensor measures the speed of the paddle wheel. The speed of the boat is then displayed on a readout. Again, this is not a direct indication of the vessel speed relative to ground, since the water is moved by current and waves.

An electromagnetic speed sensor works by generating an electromagnetic field and measuring the voltage created by a conductor passing through the field. The sensor is usually mounted on the side of the hull, with the field perpendicular to the direction of travel. As the boat moves through the water, the conductor (usually a metal plate or wire) is forced through the field, and the resulting voltage is used to determine the speed of the boat. Electromagnetic speed sensors typically deliver boat speed and log, as well as water temperature. However, they measure the water speed close to the vessel's frame, within the vessel boundary layer.

Finally, the ultrasonic technology allows anti-fouling paint to be applied to the sensor, keeping it clean all season and reducing maintenance. The electromagnetic speed sensor is the top of the range, providing highly accurate data in all waters, including low visibility conditions. It also has no moving parts and is a robust and compact device that will not create drag in the water or is unlikely to get caught on weeds or other debris. The ultrasonic sensor does not need calibration as frequently as the other sensors, either. However, one slight downside of the ultrasonic speed sensor is that it can lose a degree of accuracy in murky or dirty water.

3.2.3 Inertial Sensors

The dead reckoning function could potentially also be supplied by an inertial navigation system (INS). The performance of gyroscopes and accelerometers is typically classified into grades, as shown in Table 3-2. It is recommended to classify inertial sensors by their level of performance rather than their sensor type (microelectromechanical systems (MEMS), ring laser gyroscopes, fibre optic gyroscopes, etc.).

Grade	Acc Bias (mg)	Vel Ran Walk (m/s/ $\sqrt{hr}$)	Gyro Bias (deg/hr)	Angle Ran Walk (deg/ $\sqrt{hr}$)	INS Error 1S	INS Error 10S	INS Error 60S	INS Error 10min
Consumer	10	1	100	2	6cm	6.5m	400m	200km
Industrial	1	0.1	10	0.2	6mm	0.7m	40m	20km
Tactical	0.1	0.03	1	0.05	1mm	8cm	5m	2km
Navigation	0.01	0.01	0.01	0.01	<1mm	1mm	50cm	100m

Table 3-2 Sensor Grades and INS Error (Vectornav, [RD.12])

While inertial devices are not mandatory for SOLAS vessels, a significant number of ships incorporate an inertial measurement unit (IMU) in their station-keeping and dynamic positioning (DP) systems to mitigate noise in the GNSS data and provide more stable vessel control. Vessels engaged in bathymetric surveys also frequently equip themselves with high-quality IMU devices to enhance survey data accuracy.

Ship owners may install an inertial measurement unit (IMU) system if they deem it necessary, as IMUs are not mandatory for SOLAS vessels and are not regulated by the IMO.

The integration of an inertial measurement unit (IMU) into a comprehensive system-of-systems for resilient position, navigation, and timing (PNT) holds immense potential for SOLAS vessels. The benefits of employing an IMU are manifold:

- Provision of pitch, roll, and yaw information as well as rate of turn.
- High update rate, improved short-term position fixing, and smoothing of GNSS position fixing epochs.

- Calibration of traditional DR sensors such as magnetic compasses, and speed sensors. The latter is particularly important as seabed-sensing speed logs suffer bias errors due to vertical orientation (pitch and roll).
- Provision of a single integrated Position-Velocity solution. Ideally the vessel's position, velocity, and acceleration would be output from an IMU, and a suite of other sensors (GNSS, compass, velocity log, other radio systems) can provide input to calibrate IMU errors and biases.

The final point is especially significant because an IMU alone cannot provide accurate position or velocity data for an extended period. Standard IMU output can become unacceptably inaccurate after just a few seconds of operation without calibration. While higher-cost devices like ring laser gyros can maintain accuracy for longer durations, their cost can be prohibitive, which discourages ship owners from using them unnecessarily.

The requirement for SOLAS-class vessels to equip IMUs is not anticipated anytime soon, and the widespread adoption of navigation-grade laser gyro devices on merchant vessels is highly improbable. Consequently, this project has excluded IMU analysis as a potential sensor for the VAIM algorithm, despite its potential to provide significant added value in the future.

3.3 Assessment of GNSS and DR Loose Coupling Scheme

This section presents an evaluation and comparison of various loosely coupled GNSS and dead reckoning methods to determine the most suitable approach for the maritime environment and its specific requirements, considering the potential future need to integrate additional inputs from the resilient PNT system-of-systems.

To begin, it is essential to define which schemes fall under the umbrella of loose coupling. A loosely coupled system is characterized by weak associations between its components, such that changes in one component have a minimal impact on the existence or performance of another component. In the context of GNSS, loosely coupled schemes are those where the positions and velocities derived from GNSS signal processing are merged as updates to the positional/velocity information estimated by other sensors.

In this specific instance, considering the sensors outlined in section 3.2, the loose coupling technique merges the positioning and velocity data provided by GNSS with the heading, positioning, and/or velocity information provided by the DR sensors.

It is crucial to bear in mind the objective of this work package, which is to develop a robust integrity concept for VAIM by integrating dual-frequency, multi-constellation GNSS and dead reckoning, with the potential to incorporate additional inputs in the future. While this chapter outlines various available concepts, the safest and most technology-agnostic approach will be selected for INSPIRe VAIM.

3.3.1 PVT Coherence Test

This section outlines the fundamental principle underlying the high-level PVT coherence test. The concept involves comparing the positioning and velocity data provided by two distinct sensors to determine whether the information they provide is consistent. This may be the first and the simplest integrity concept for loose-coupling hybridisation.

Conceptually, this approach is straightforward. When the position estimates provided by GNSS and the independent dead reckoning system diverge significantly, an alarm is triggered, indicating that one of the systems (likely GNSS) is delivering inaccurate information.

The concept relies on the definition what is considered as "too separated" and to define a threshold for a positioning/velocity difference. An appropriate characterisation of devices nature selected would allow the usage of statistical tools such as hypothesis contrasts, which

can be configured for different levels of confidence and therefore an integrity risk can be derived.

The principle consists of calculating the information from these two or more sensors and evaluating the difference between them. If the difference between them is big enough this test will alarm to avoid using the position solution. On the other case the probability that this error is not detected will be lower than a configured PMD (Probability of Miss Detection) value.

Finally, this test could be performed for the difference of vessel state provided by two or more sensors. The difference relies on the capability to detect which is the sensor that most likely is experiencing the error. Therefore, the following options are available:

- FD PVT Coherence Test: the test is performed for the difference in the state provided by two sensors. When the alarm is raised there is no way to identify the failing system, and therefore a don't use alarm will be raised impacting positioning availability.
- FDE PVT Coherence Test: the test is performed for the difference in the state provided by more than two sensors. Then, FD PVT Coherence Test could be performed for each state pairs. If all the test where one of the sensors raise alarms, then it is very likely that that sensor is the one whose state is faulty, and therefore could be excluded from the solution.

This is the main principle of PVT coherence test, more complex architectures using the same basic principle could be developed. For the potential usage in the INSPIRe VAIM concept the following advantages and disadvantages are identified:

- Benefits:
  - It can provide a test with a probability that the error is not detected lower to a configurable value.
  - It can identify the faulty sensor if more than two sensors are considered in the architecture.
  - It is the first and simplest concept available for GNSS hybridisation with DR sensors regarding fault detection.
  - It could be used in combination with other concepts since it only provides an alarm when a failure is detected.
  - It is aligned with the IMO/MSC.401(95) [RD.3] concept where state and integrity information is provided to a central processing element, and further integrity checks could be performed on top.
- Drawbacks:
  - It requires a safe characterisation of a fault-free error distribution for each of the sensors involved.
  - It is not able to provide a combined estimation of the state with the information from the different sensors, since it only provides alarms.
  - In order to configure the test threshold, it requires the definition of a parameter called MDE (Minimum Detectable Error) which is the minimum size of difference between status able to be detected with the probability configured.

3.3.2 GNSS state vector propagation

The second concept for a GNSS loose coupling with a DR sensor, not exclusive from the previous one, is the capability to propagate previous GNSS safe state and provide an error bounding for the propagation.

The principle is quite simple from the conceptual point of view. The safe state estimation of the GNSS solution selected in preliminary epoch is propagated employing the measurements received from the DR sensors. This approach is the simplest possible architecture to provide a combined hybridised solution.

Furthermore, the same principle could be applied to the incertitude of the state estimation, which could be propagated if the incertitude of the DR propagation is also bounded. As an example, the positioning accuracy (ACC95) or the positioning bounding (PL) of the GNSS solution selected in previous epoch is increased to ensure that the PL considers and bounds the GNSS position and the propagation errors. The amount in which these parameters will have to be increased will depend on the time elapsed and on the quality of the sensors.

In order to compute this additional bounding of the error propagation, to be added to the GNSS one, it is necessary to characterise the propagation error incertitude. This characterisation is key, and safety related in this scheme.

This concept then will improve the performances, the vessel can pass in a short period of time from open-sky or good visibility conditions to harsh conditions (e.g., in port navigation), in such situation the previous propagated ACC95/PL can be lower than the one computed at that epoch. The objective of proposed approach is to try to reduce the impact on the availability caused by such conditions and maximise the performances.

This optimisation of the performance could be then done selecting the smallest ACC95/PL from all the valid ones from the sliding window propagated to the current epoch. Then, the estimated location is the one associated to that minimum ACC95/PL.

This is the main principle of GNSS state vector propagation, more complex architectures using the same basic principle could be developed. For the potential usage in the INSPIRe VAIM concept the following advantages and disadvantages are identified:

- Benefits:
  - It can provide a safe bounding of the state incertitude up to a configurable value.
  - It can provide a combined estimation, using all the sensors considered in the architecture, optimising the performances.
  - It is the first and simplest concept available for GNSS hybridisation with DR sensors regarding state estimation.
  - It could be used in combination with other concepts, since it does not provide any alarm for a failure detection.
  - It is aligned with the IMO/MSC.401(95) [RD.3] concept where state and integrity information are provided to a central processing element and combined for a single state estimation and integrity provided to mariner.
- Drawbacks:
  - It requires a safe characterisation of error distribution for each of the sensors involved in order to compute a safe estimation bounding.
  - It is not able to provide fault alarms. However, estimation bounding could be inflated on real time providing evidence that something is wrong.

- Quality of the sensors drives the performances of the concept, and they could be not enough for some navigation phases.

3.3.3 Kalman Filter DR-GNSS loose coupling

Finally, the most common approach for a GNSS loose coupling with a DR sensor is the usage of a Kalman Filtering (KF) algorithm. In this approach the GNSS provides an independent position/velocity solution, which is then combined with the IMU and/or odometer PVT solution in order to provide an integrated solution.

The DR measurements are used to measure the change in position and velocity at a high rate between GNSS measurement epochs by using the same mechanization equations as in the uncoupled approach. Then whenever there is a new GNSS measurement epoch (in general, once a second), a new GNSS solution is computed (either snapshot or filtered solution) and combined with the DR solution in a Kalman Filter to find the optimal solution.

The principle is quite simple from the conceptual point of view. The safe state estimation of the GNSS solution selected in preliminary epoch is propagated employing the measurements received from the DR sensors. This approach is the simplest possible architecture to provide a combined hybridised solution.

The approach is well known and there is a huge amount of literature available with different sensors architecture following the same principle. However, how to safely bound the incertitude of the state vector is under investigation, and few solutions have demonstrated the safety.

One of the possibilities is the integrity architecture presented in [RD.14] for a GNSS/IMU navigation system, which could be exported to other DR sensors. The architecture exploits the existing GNSS integrity systems to guarantee the required levels of integrity against GNSS failures. In this study, the WLS-RAIM algorithm, which is the most typical and computationally efficient form of integrity monitoring, is applied for a GNSS integrity monitoring algorithm. In addition to the GNSS system failure, this study newly proposes an integrity assurance against IMU sensor failures to fully assure the total navigation system integrity of the integrated system. The total navigation system integrity is assured by computing the Extended Kalman Filter (EKF) PLs for each fault hypothesis.

The fault-free EKF PLs is estimated by the KF variance, which requires a safe bounding of the process noise variance. The EKF PLs for each fault requires a bounding of the worst-case bias and the nominal variance provided by the FK, and therefore a full knowledge of the fault tree and the characterisation of these potential errors.

The concept presented in [RD.14] is not necessarily the most suitable one for INSPIRe VAIM. Is just an example to highlight that integrity and positioning error bounding could not directly estimated from the KF estimated variance.

This is the main principle of KF loose-coupling integrity concept, more complex architectures using the same basic principle could be developed. For the potential usage in the INSPIRe VAIM concept the following advantages and disadvantages are identified:

- Benefits:
  - It can provide a safe bounding of the state incertitude up to a configurable value.
  - It can provide a combined estimation, using all the sensors considered in the architecture, optimising the performances.
  - It is the most used algorithm for GNSS hybridisation with DR sensors regarding state estimation, therefore there is a lot of research and literature available.
  - It could also provide alarm for a failure detection.

- It is aligned with the IMO/MSC.401(95) [RD.3] concept where state and integrity information are provided to a central processing element and combined for a single state estimation and integrity provided to mariner.

- Drawbacks:
  - It requires a safe characterisation of error distribution for each of the sensors involved to compute a safe estimation bounding.
  - It requires a deep knowledge of the failure tree and characterisation of the potential errors.
  - It could be computationally demanding.
  - It may be required to make assumptions about distributions of faulty errors. As an example, the concept presented in [RD.14] relies on assumption of the measurement noise obeying a normal biased distribution.

4 HIGH LEVEL ALGORITHM DESIGN

This section provides a high-level design for the VAIM algorithm developed on top of the already detailed M(G)RAIM algorithms.

4.1 Mathematical Description

Following chapters will provide a high-level description of the different VAIM modules. However, the main information flow and relationship between modules is detailed in the following chart.

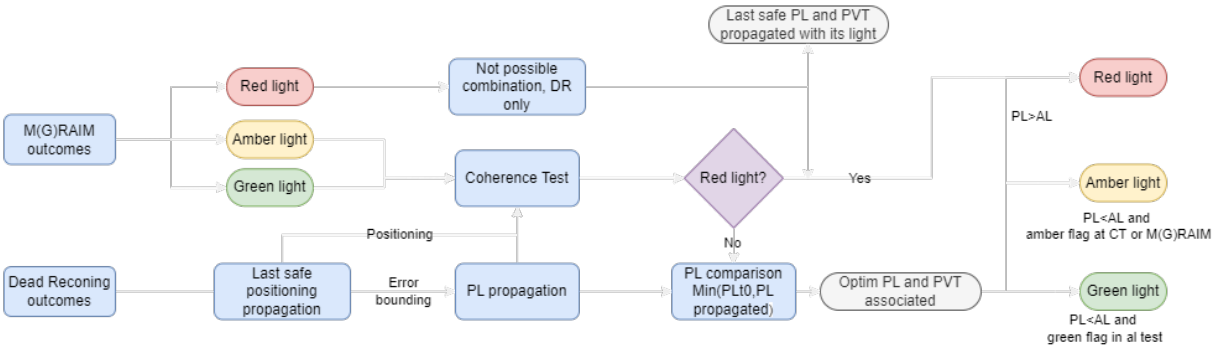

Figure 4-1. VAIM conceptual flowchart

The chart is depicted for a single epoch processing. VAIM algorithm considers the propagation could be made not only from the previous epoch, but for sliding window. Then, VAIM algorithm will select those with the best performances (minimum PL or ACC95) and its associated PVT information.

4.1.1 Positioning estimation before loose coupling

We consider the mathematical process of providing a safe positioning taking into account the information of the positioning and the quality metrics given by GNSS and the other sensor combinations detailed in section 3.2.

From GNSS M(G)RAIM algorithm the following information will be required:

- Estimated location.
- A_{95} or HPL, depending on the algorithm selected.
- Integrity flag from M(G)RAIM

From non-GNSS device combination the following information will be required:

- Estimated location from the GNSS safe positioning (t-N) epochs ago, where N is a sliding window.
- A_{95} or HPL from the hybridisation technique selected.

This information will allow VAIM algorithm to implement the following two concepts on top of the M(G)RAIM algorithms.

4.1.2 Coherence Test

This section aims to detail the coherence test concept. The idea is to compare the two position estimates provided by different sensors to assess whether the information they provide is consistent, or coherent. This may be the first and the simplest integrity concept for hybridisation.

From a general perspective, this concept could be easily understood. When the positioning provided by the GNSS and the positioning provided by the dead reckoning system are too

separated, an alarm is raised because one of them (likely the GNSS) is providing misleading information.

The issue is then to evaluate what is considered as “too separated” and to define a threshold. An appropriate characterisation of devices nature selected would allow the usage of statistical tools such as hypothesis contrasts, which can be configured for different levels of confidence and therefore an integrity risk can be derived.

The principle consists of calculating both the position solution and evaluating the difference between them. If the bias between them is big enough this test will alarm to avoid using the position solution. On the other case the probability that this error is not detected will be lower than a value PMD (Probability of Miss Detection).

In order to make this example simpler, assumptions that 1D position is given and that the error distribution of both systems is Gaussian are made. This analysis then could be made for the horizontal segment that joins the GNSS and the dead reckoning location.

The figure below represents the probability distribution of the positioning difference for fault free (blue) and a faulty (orange) case, where one of the systems (i.e., GNSS) would be moved from the actual position, which means a significant bias with respect to the other. Then, a threshold is set in each point that under nominal conditions the alarms are below a given rate (area below blue curve is equal or less than PFA, Probability of False Alarms). As the system under a failure condition is biased, the probability that a measurement is below the threshold would be equal or less than the PMD. The distance between the mean of both solutions is known as the MDE (Minimum Detectable Error).

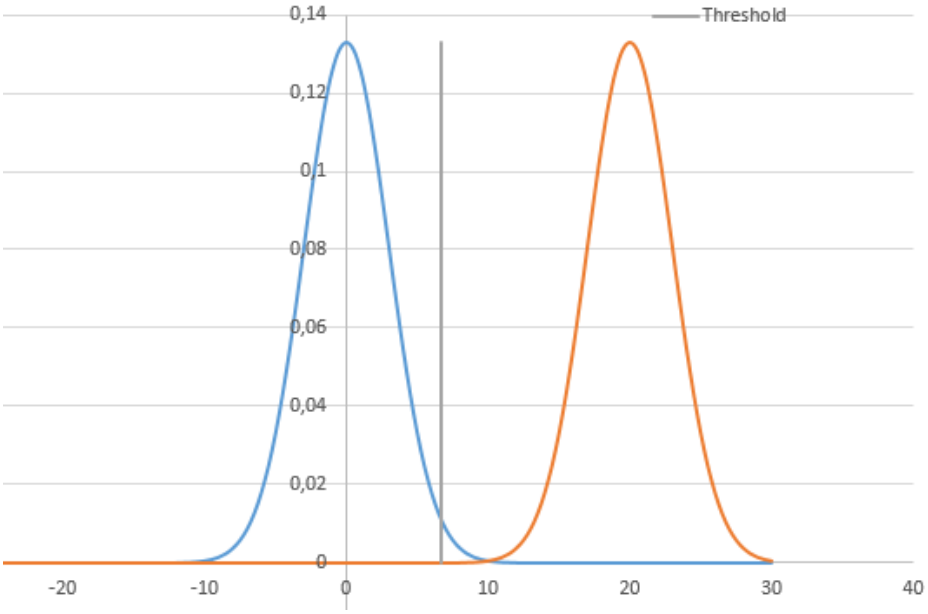

Figure 4-2. Position Domain Consistency Check. The plot represents the difference in the positioning for fault-free case distribution function (blue line) and faulty case distribution function (orange line).

Once the Threshold is calculated given the typical accuracy of the first positioning estimation and the PFA, positioning will be measured to assess if the separation is over or below the threshold and provide the necessary integrity alarms.

In addition to that, with the typical accuracy of the second sensor and the IR/PMD it will be defined the necessary bias for a faulty case to fulfil that requirement. Therefore, it will be provided a MDB (Minimum Detectable Bias) on real time about what is the smallest error could be detected with that IR/PMD. This is the indeed a limitation in the bias detection capability, errors smaller than MDB cannot be detected with the requested probability, and they may cause integrity breaks.

If this test is made propagating the position only from the last GNSS positioning, only step errors could be detected. Therefore, it is proposed to perform this test iteratively propagating the positioning from the last N epochs to the current one, in order to detect also potential ramp errors.

Taking this concept into consideration, the following integrity flag concept is proposed:

- In case any alarm is raised (positioning difference over the threshold), the overall positioning will be flagged as red and no safe positioning will be provided.
- In case no alarm is raised (positioning difference below the threshold), but the largest MDB is larger than the required accuracy, an amber flag will be raised.
- A green flag will be raised when no alarm is detected (positioning difference below the threshold) and the largest MDB is smaller than the required accuracy.

4.1.3 GNSS state vector propagation

The second concept for a GNSS loose coupling with other sensor, not exclusive from the previous one, is the capability to propagate previous GNSS safe positioning and provide an error bounding, in a similar way as ACC95 and PL do.

The position of the GNSS solution selected in previous epoch is propagated employing the measurements received from the alternative sensors since the previous safe epoch considering the status now when the solution was generated. The propagation of the position will be detailed in the D4.1 Algorithm definition [RD.13].

Then, the positioning accuracy (ACC95) or the positioning bounding (PL) of the M(G)RAIM solution selected in the previous epoch is increased to ensure that the PL considers and bounds the position propagation errors. The amount in which these parameters will have to be increased will depend on the time passed from the moment when the previous selected solution was generated, on the quality of the sensors and on the initial errors.

In order to compute this additional bounding of the error propagation, to be added to the ACC95 or the PL, the following steps shall be performed, the detailed implementation is specified in the D4.1 Algorithm definition [RD.13].

- Compute the overbounding of the velocity errors, at each Δt propagation step based on the sensor error overbounding parameters.
- Based on the overbounding of the velocity errors, the user velocity and the overbounding of the initial heading error, compute the heading angle error bound after *k* propagation steps corresponding to the TIR
- Based on the overbounding of the velocity errors, the user velocity and the overbounding of the heading, obtain the increment of PL for the corresponding TIR or the propagation of the ACC95 due to the propagation of k steps

The vessel can pass in a short period of time from open-sky or good visibility conditions to harsh conditions (e.g., in port navigation), in such situation the previous propagated ACC95/PL can be lower than the one computed at that epoch. The objective of proposed approach is to try to reduce the impact on the availability caused by such conditions and maximise the performances.

This optimisation of the performance is then done selecting the smallest ACC95/PL from all the valid ones from the sliding window propagated to the current epoch. Then, the estimated location is the one associated to that minimum ACC95/PL.

If this test is made propagating the position only from the last GNSS positioning, only step errors could be detected. Therefore, it is proposed to perform this test iteratively propagating

the positioning from the last N epochs to the current one, in order to detect also potential ramp errors.

Taking this concept into consideration, the following integrity flag concept for each epoch is proposed:

- A red light will be raised:
  - In case any alarm is raised by M(G)RAIM, or the coherence test detailed in section 4.1.2 if used before this algorithm.
  - The overall ACC95 or PL is larger than the defined threshold.
- Amber flag will be raised if an amber flag is raised by the M(G)RAIM, or the coherence test detailed in section 4.1.2 if used before this algorithm.
- A green flag will be raised when no alarm is detected and the propagated ACC95 or PL remains under the configured threshold for the navigation phase.
- In case that for the given epoch a red or amber flag is raised, the sliding window allows the user to provide the last safe positioning propagated to the given epoch.

4.1.4 Summary

Following this process, the following output states may be applicable.

Table 4-1: Summary of VAIM integrity algorithm output states per epoch

M(G)RAIM	Coherence test	PL from M(G)RAIM	PL propagated	PL selected	Status Flag	PL and position from
RED	N/A	N/A	PL Propagated from previous green flag epoch	Min(PL propagate from green flag epoch)	RED	From purely propagation from green flag epoch
AMBER	RED	PL M(G)RAIM	PL Propagated from previous green flag epoch	Min(PL propagate from green flag epoch)	RED	From purely propagation from green flag epoch
AMBER/ GREEN	AMBER/ GREEN	PL M(G)RAIM	PL Propagated with epoch information and from previous green flag epoch	Min(PL M(G)RAIM; PL Propagated) >AL	RED	From M(G) RAIM or propagated
AMBER	AMBER/ GREEN	PL M(G)RAIM	PL Propagated with epoch information and from previous green flag epoch	Min(PL M(G)RAIM; PL Propagated) ≤AL	AMBER	From M(G) RAIM or propagated
AMBER/ GREEN	AMBER	PL M(G)RAIM	PL Propagated with epoch information and from previous green flag epoch	Min(PL M(G)RAIM; PL Propagated) ≤AL	AMBER	From M(G) RAIM or propagated
GREEN	GREEN	PL M(G)RAIM	PL Propagated with epoch information and from previous green flag epoch	Min(PL M(G)RAIM; PL Propagated) ≤AL	GREEN	From M(G) RAIM or propagated

5 DESCRIPTION OF ALGORITHM TESTING

This section presents an overview of the experimentation plan for the evaluation of the algorithm and a summary of the results of algorithm testing. The sections that follow then go into more detail on each element. The purpose of the experimentation is to assess the MGRAIM algorithm developed.

The experimentation consists of the following sequential stages:

- Data collection & generation
- Data processing
- Performance evaluation

These stages are discussed in the following subsections.

5.1 Data Generation and Data Processing

The functional testing and performance evaluation was executed based on the collection of real GNSS data (GPS and Galileo observables), within GMV archives.

5.1.1 GNSS Data

GNSS Data are measured with the Septentrio PolarRx5S. The PolaRx5S from Septentrio is a high-performance GNSS receiver capable of multi-constellation position solutions and logging, at a maximum of 100Hz. Supported constellations include GNSS DFMC, L2, L5, Galileo E1, E5 (a, b, AltBoc) E6, BeiDou, B1, B, B3 and SBAS.

The data was collected on October 19, 2021, in the fjord at Trondheim, Norway. The survey commenced at 8:00 AM and was executed over a duration of two hours. This test scenario involves piloting the vessel into the open water of the fjord. This test trajectory is shown in Figure 5-1. This test scenario also covers the coastal phase of the voyage due to the vessel not travelling further than 50 nautical miles away from the nearest coast however this test covers more of an open water type of scenario. The total planned voyage is ~12.5 miles.

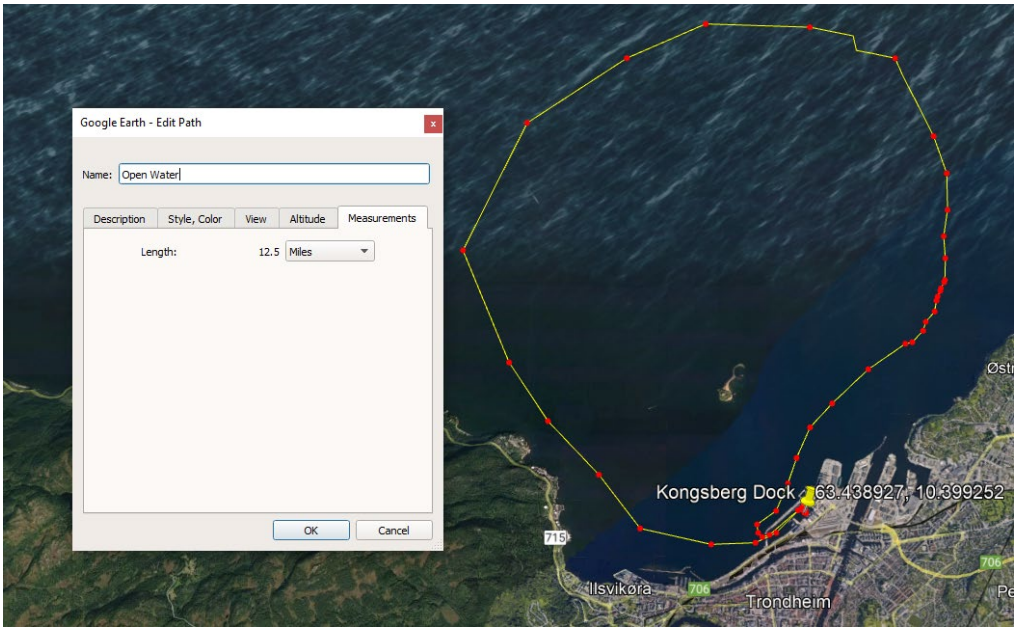

Figure 5-1: Open water test trajectory.

The GNSS equipment was installed on board a vessel as part of the testbed for the collection and evaluation of a services under real-life conditions representative of the environment for the final intended service to the mariner. On board the vessel there were three GNSS antennas the NavXperience 3G+C maritime antennas mounted at fixed points on the vessel along a metal bar along the starboard (right-hand) side of the vessel. These mounting points are 2 meters apart from each other. The front and back antennas will be connected to the AsteRx 4 to provide GNSS based attitude and the central antenna will be used for the PolaRx 5S and USRP. The antenna placement is shown in Figure 5-2 below:

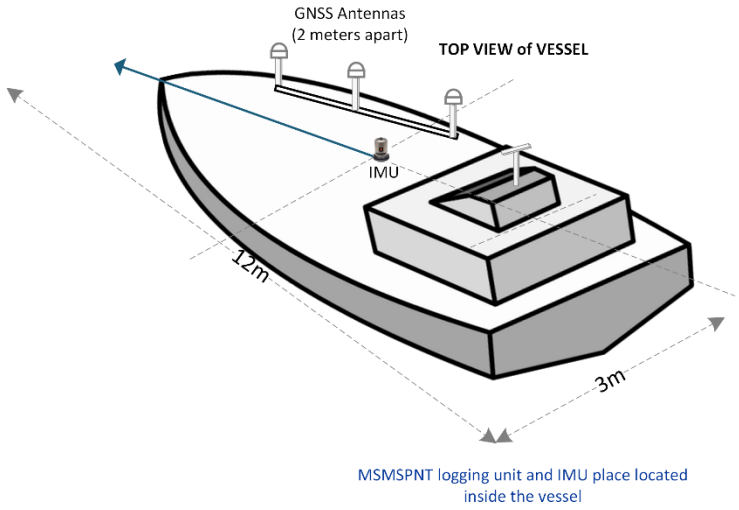

Figure 5-2: Antenna roof placements.

Table 5-1 below provides a summary of the data collected for analysis.

Table 5-1 GPS Data collected for analysis

Date	Duration		Constellation/Frequency	File Format	Conversion Tool
	From	To			
October 19, 2021	8:03:10.am	10:05:30	GNSS DFMC/L5 GAL E1/E5	RTKCONV 2.4.3	RTKCONV 2.4.3

5.1.2 SBAS Data

The EGNOS data used within this project was retrieved from GMV NSL's internal archive, in the EMS format. Table 5-2 below provides a summary of the data collected for analysis.

Table 5-2 EGNOS Data collected for analysis

Date	Duration		PRN	File Format	Conversion Tool
	From	To			
October 19, 2021	08:00:00	11:00:00	123	EMS	GMVNSL EMS Decoder

5.1.3 Simulation Data Generation

Simulated data provides an option to cover scenarios that would otherwise not be possible using field data alone. Table 5-3 provides the specification for the Threats and Faults which are applicable to and will be used to develop the INSPIRe integrity solutions. To facilitate the analysis of these faults on the positioning solution, GMV has created a series of functions to

introduce the errors to the RINEX files in a coherent way for a DF combination. Multiple faults for each of these scenarios are created by introducing ramps or biases or multipath on multiple satellites at the same time.

Table 5-3 Fault Injection

Fault	Baseline Function	Notes
Satellite Clock failure (ramp)	The fault injection tool applies a ramp error on a specified satellite	Standard clock failure on a single satellite – determined to be a steady clock ramp on one measurement.
Satellite Clock failure (bias)	The fault injection tool applies a bias value to a single SV	Clock failure on a single satellite leading to a bias/offset.
Satellite Bad Ephemeris Upload	Modification of parameters in the navigation message	Single satellite failure due to a bad ephemeris upload results in incorrect information.
Satellite multipath	The fault injection tool applies an elevation-dependent error is added to each pseudo range observation, with a random noise component included	Multipath induced error on a single satellite e.g., the introduction of oscillating bias error. Typical of a maritime environmental hazard.

Additionally, the speed log and compass measurements used in this WP for the VAIM analysis were simulated through the reference solution with addition Gaussian noise.

5.1.4 Data Processing

The collected data will be processed off-line and in non-real time using the algorithm and several supporting tools. A set of algorithm performance test scenarios are defined in Section 5.2. The following high-level processing step shall be carried out:

- Run TPDF for each test scenario, configured according to test scenario definition.
  - Inputs:
    - RINEX observation file and navigation file
    - If SBAS legacy mode:
      - *.csv files output by EGNOS decoder for applicable calendar day.
    - Speed log and compass
      - Velocity in horizontal
      - Heading
  - Outputs:
    - PVT results files (.csv)
    - SBAS engine (Legacy)
    - M(G)RAIM engine
  - Residual data files (.csv)

5.2 Test Scenarios

A set of 24 test scenarios has been defined, as described in the table below.

Table 5-4 Test Scenarios

Test Scenario	Correction mode	Fault injection	Smoothing time constant
TS.01	MGRAIM GNSS DFMC	None	100s
TS.02	MRAIM GNSS DFMC	None	100s
TS.03	MGRAIM GNSS DFMC(VAIM enabled)	Single Satellite Clock failure (ramp) - High Elevation SV	100s
TS.04	MRAIM GNSS DFMC(VAIM enabled)	Single Satellite Clock failure (ramp) - High Elevation SV	100s
TS.05	MGRAIM GNSS DFMC(VAIM enabled)	Multiple Satellite Clock failure (ramp) - High Elevation SV	100s
TS.06	MRAIM GNSS DFMC(VAIM enabled)	Multiple Satellite Clock failure (ramp) - High Elevation SV	100s
TS.07	MGRAIM GNSS DFMC(VAIM enabled)	Single Satellite Clock failure (bias) - High Elevation SV	100s
TS.08	MRAIM GNSS DFMC(VAIM enabled)	Single Satellite Clock failure (bias) - High Elevation SV	100s
TS.09	MGRAIM GNSS DFMC(VAIM enabled)	Multiple Satellite Clock failure (bias) - High Elevation SV	100s
TS.10	MRAIM GNSS DFMC(VAIM enabled)	Multiple Satellite Clock failure (bias) - High Elevation SV	100s
TS.11	MGRAIM DFMC	Single Satellite Bad Ephemeris Upload - High Elevation SV	100s
TS.12	MRAIM DFMC	Single Satellite Bad Ephemeris Upload - High Elevation SV	100s
TS.13	MGRAIM GNSS DFMC(VAIM enabled)	Multiple Satellite Clock failure (ephemeris) - High Elevation SV	100s
TS.14	MRAIM GNSS DFMC(VAIM enabled)	Multiple Satellite Clock failure (ephemeris) - High Elevation SV	100s
TS.15	MGRAIM DFMC	Applying multipath error on a single high-elevation SV	100s
TS.16	MRAIM DFMC	Applying multipath error on a single high-elevation SV	100s
TS.17	MGRAIM GNSS DFMC(VAIM enabled)	Applying multipath error on a Multiple GPS high-elevation SV	100s
TS.18	MRAIM GNSS DFMC(VAIM enabled)	Applying multipath error on a Multiple GPS high-elevation SV	100s

6 EVALUATE THE ALGORITHM

This section describes the testing and evaluation of the prototype algorithms within a simulated test environment using real-world data, aimed at assessing the algorithm's suitability for its intended purpose.

The algorithm assessment was executed using the algorithm design described in Section 4 for both single and multiple satellite faults. Here the algorithms' ability to detect GNSS faults and where applicable exclude the faults as described in Section 5.1.3 and to raise the appropriate alert as defined in Section 4 was analysed.

Figure 6-1 depicts the satellite visibility for the selected dataset. The blue window highlights the period during which the fault was injected into the high satellite G01 (elevation: 76°, azimuth: 188°). This satellite was used for executing the single-fault test cases. The fault was injected at t=844s (SOW: 202634s) for a period of 300s, ending at t = 1144s (SOW: 202934s).

For the multiple satellite fault analysis, the injection was done using G01 and a second satellite, G04 (elevation: 52°, azimuth: 184°). The fault was injected on G04 from t=2558s (SOW: 204348s) to t = 2858s (SOW: 204648s). Any additional faults detected by the algorithm outside the specified time periods of the injected faults are considered inherent to the data and have not been fully analysed to determine their origin and root cause.

The results presented later in this section are for single and multiple satellite fault case according to the test scenarios defined in Section 5.2.

Figure 6-1 Satellite visibility condition and Fault injected on satellite G01 at time = 08:16:56 (844s) to 08:21:26 (1144s) and G04 at time = 08:45:30 (2558s) to t = 08:50:30 (2858s)

It should be noted that for illustrative purposes for results where faults are injected, and the red integrity flag is raised the horizontal error is plotted to show the potential effect of the fault, but the position is not provided in such a case.

The computation of the fault detection and FDE processes for the MGRAIM and MRAIM algorithm respectively are described in full details in [RD.13].

The integrity warning outputs that are provided in the results plotted below illustrates one or a combination of the following traffic light indicators, the flag carry the following meaning:

- MGRAIM
  - Red light: provided to the mariner when at least one of the availability check or the fault detection test do not pass.

- Amber light: provided to the mariner when geometry screening raises an alarm for at least one subset.
- Green light: provided to the mariner when all the tests are performed successfully, and the solution is therefore suitable for navigation.

- MRAIM
  - Red light: provided to the mariner when the HPL (no fault or fault excluded) or Horizontal Uncertainty Level (HUL) (fault detected and not excluded) is computed and it is above the HAL.
  - Amber light: provided to the mariner when there is not enough satellite available to create subsets and provide a solution for every subset and the integrity requested.
  - Green light: provided to the mariner when the HPL (no fault or fault excluded) or HUL (fault detected and not excluded) is computed and it is below the HAL and no faults are detected.

The M(G)RAIM alarm management in VAIM algorithm is as follows for each of the epochs of the sliding window:

- M(G)RAIM red light: VAIM algorithm modules are not processed and **red light is provided directly** for that epoch.
- M(G)RAIM amber light: VAIM algorithm modules are processed normally, and amber or red light is provided for that epoch, depending on the VAIM outcomes. A **green light could never be provided**.
- M(G)RAIM green light: VAIM algorithm modules are processed normally, **and green, amber or red light is provided** for that epoch, depending on the VAIM outcomes.

6.1 Presentation of Experimentation and Evaluation results

6.1.1 Evaluation of a Fault-free Dataset

This subsection shows the results generated using a smoothing constant of 100 seconds based on the following test scenario:

Test Scenario	Correction mode	Fault injection
TS.01	MGRAIM DFMC	none
TS.02	MRAIM DFMC	none

6.1.1.1 TS01 – PVTI Performance Analysis (MGRAIM DFMC)

Figure 6-2 show fault detection test results from Test Scenario 01 MGRAIM DFMC. Figure 6-2 illustrates test statistics and threshold values computed for the solution generated for the dataset. Figure 6-3, shows integrity flags and the horizontal errors within the solution generated.

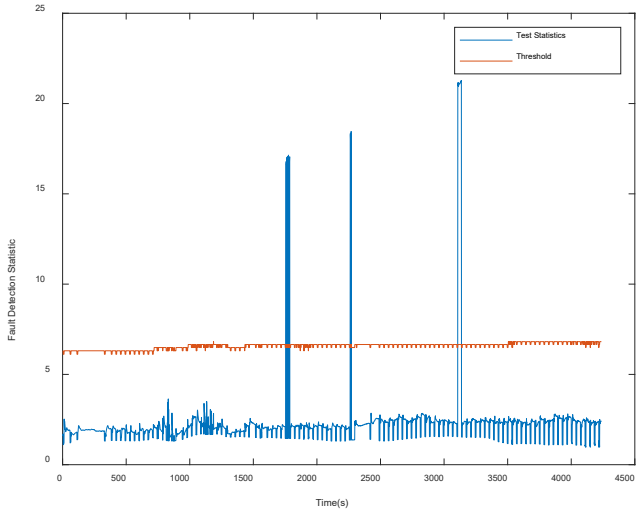

Figure 6-2 FD results from MGRAIM in fault-free case

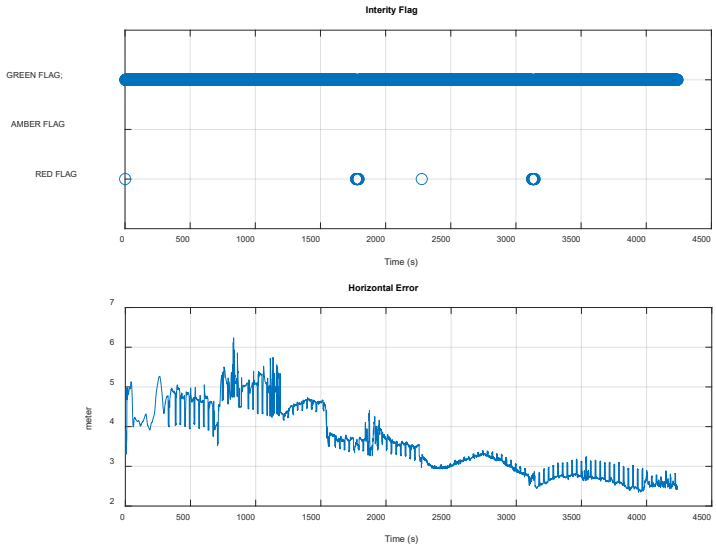

Figure 6-3 The MGRAIM DFMC Integrity Flag (above) Horizontal Error (below)

The solution performance is summarised in Table 6-1, for GNSS DFMC:

Table 6-1 TS01 - Horizontal error parameters for GNSS DFMC

	MEAN (m)	**STD(m)**	**95%(m)**
Horizontal Error (MGRAIM)	3.677	1.295	5.76

Figure 6-4 illustrate the number of satellites used to compute the PVT solution and the computed DOP.

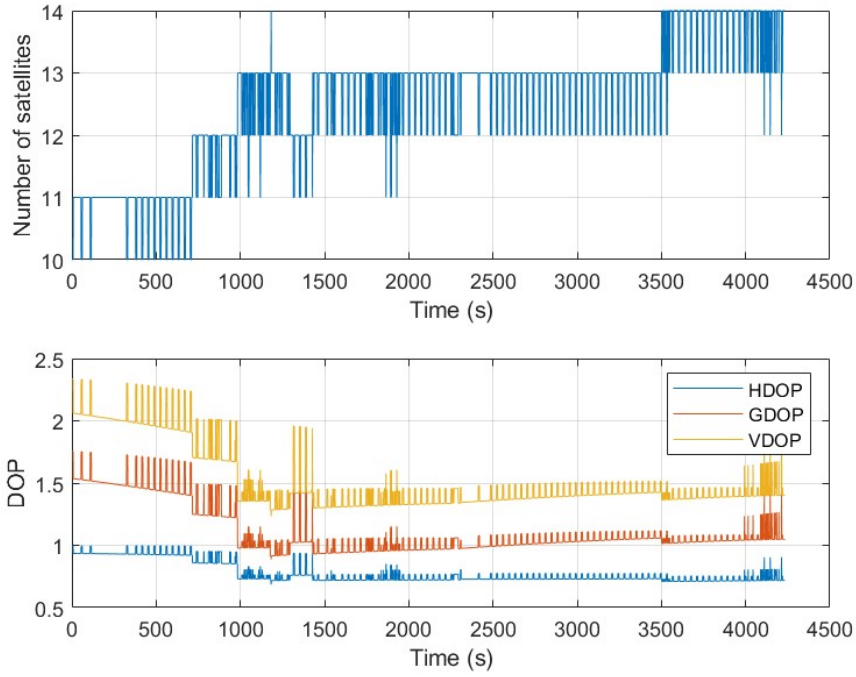

Figure 6-4 Number of SV used to generate the PVT solution and the DOP Values

6.1.1.2 TS02 – PVTI Performance Analysis (MRAIM DFMC)

Figure 6-5, shows integrity flags, the horizontal errors and the protection level generated. It can be seen from the integrity flag plot that the GREEN flag is raised which in this case indicates that the following condition was met PL< AL, the alert limit is set to the value of 25 m.

All epochs shall be green due to a great AL value, under the MRAIM algorithm if the faults can be detected but could not be excluded, the uncertainty level is estimated and compare against the predefined AL. If the UL is less than the AL value GREEN flag raised otherwise Red Flag will be raised. This will be reflected in many of the results presented in this assessment since AL is set to 25m.

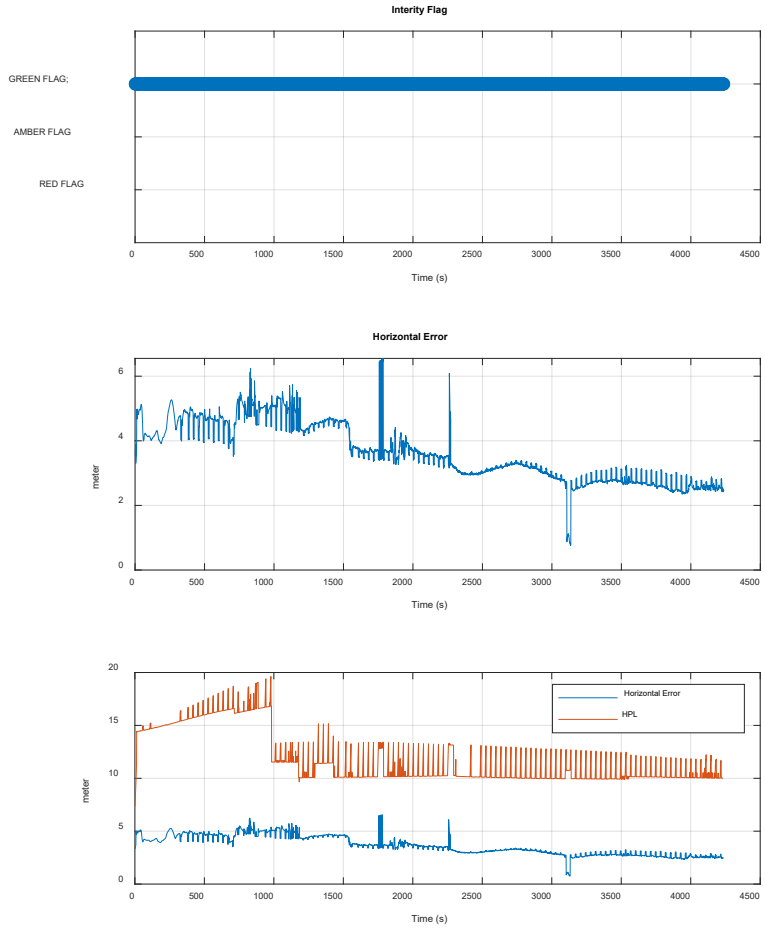

Figure 6-5 The MRAIM Integrity Flag (above), Horizontal Error(middle) and Horizontal Error vs HPL (below)

The solution performance is summarised in Table 6-2. For GNSS DFMC the horizontal error is 5.76m with a percentile of 95%.

Table 6-2 TS02 – MRAIM Fault-free case: Horizontal error parameters for GNSS DFMC

	MEAN (m)	**STD(m)**	**95%(m)**
Horizontal Error (MRAIM)	3.663	1.246	5.76

Figure 6-6 illustrate the number of satellites used to compute the PVT solution and the computed DOP.

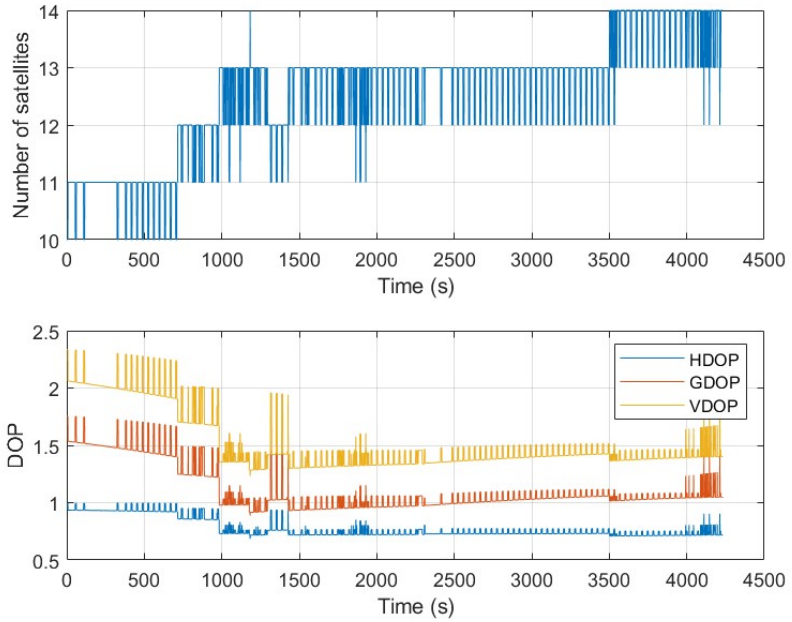

Figure 6-6 Number of SV used to generate the PVT solution and the DOP Values

6.1.2 Evaluation of GNSS Data with injected Ramp Error

6.1.2.1 Single High-elevation SV

The ramp-type fault refers to the slowly varying cumulative error which might be resulted in a jump in frequency and drift in the phase of the satellite clock. This subsection shows the results generated using a smoothing constant of 100 seconds based on the following test scenario:

Test Scenario	Correction mode	Fault injection	Comment
TS.03	MGRAIM DFMC (VAIM enabled)	Single Satellite Clock failure (ramp) - High Elevation SV	apply ramp error on a single high-elevation SV
TS.04	MRAIM DFMC (VAIM enabled)	Single Satellite Clock failure (ramp) - High Elevation SV	apply ramp error on a single high-elevation SV

Table 6-7 shows the configuration parameters and values used to create the ramp fault injection dataset. The ramp error at the speed of 0.4m/s is injected into the original pseudo-range of a single satellite from t=844s (SOW: 202634s) for a period of 300s to end at to t = 1144s (SOW: 202934s).

Table 6-3 TS03/TS04 Configuration

Parameter	Value	Comment
Start time [GPS Week SOW]	[2180 202634]	represents the time and duration of the injection of the fault
End time [GPS Week SOW]	[2180 202934]	
Constellation	['G'];	The constellation which is affected
PRN	[1];	Satellites in which the fault was injected
Range drift	[0.4m/s]	

6.1.2.1.1 TS03 – PVTI Performance Analysis (MGRAIM GNSS DFMC: VAIM enabled)

Figure 6-7 show fault detection test results from Test Scenario 03 MGRAIM GNSS DFMC. Figure 6-7 illustrates test statistics and threshold values computed for the solution generated for the dataset. The test statistics and threshold values are used within Fault Detection Test. It can be seen from the graph the point at which the test statistic exceeds the detection threshold, when this occurs the “red light” integrity alarm/flag is raised. Figure 6-8, shows integrity flags and the horizontal errors within the solution generated.

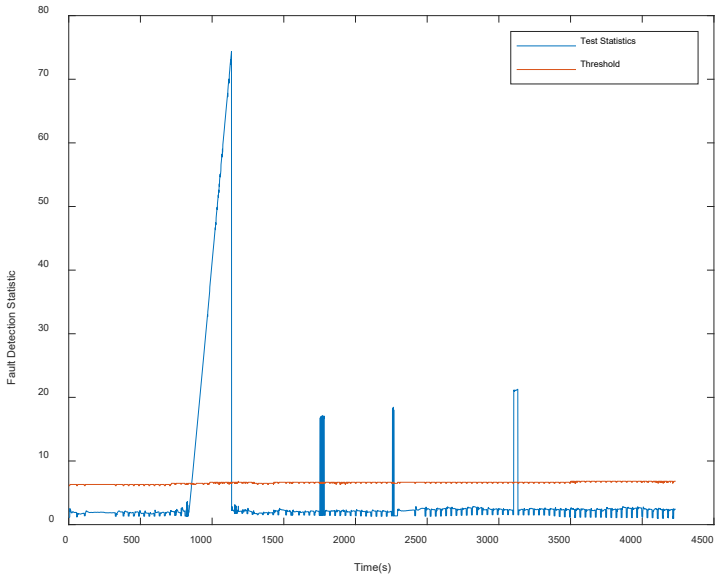

Figure 6-7 FD results from MGRAIM in Ramp fault case

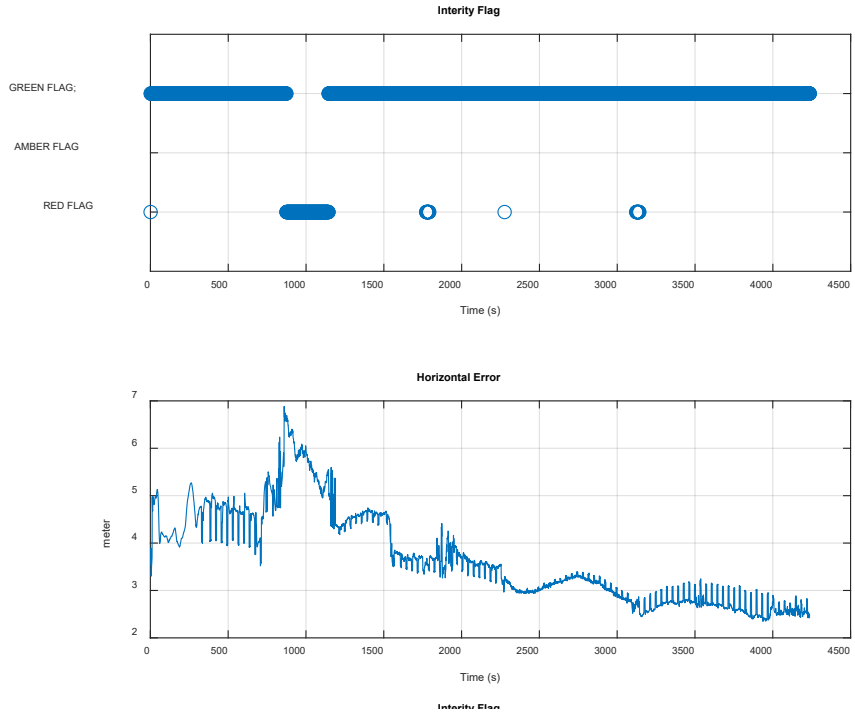

Figure 6-8 MGRAIM Integrity Flag (above) Horizontal Error (below)

The solution performance is summarised in Table 6-8 for GNSS DFMC:

Table 6-4 TS03 – Horizontal error parameters for GNSS DFMC

	MEAN (m)	STD(m)	95%(m)
Horizontal Error: VAIM enabled	3.69	2.59	5.48
Horizontal Error: MGRAIM only	3.97	2.05	6.89

Figure 6-9 illustrate the number of satellites used to compute the PVT solution and the computed DOP.

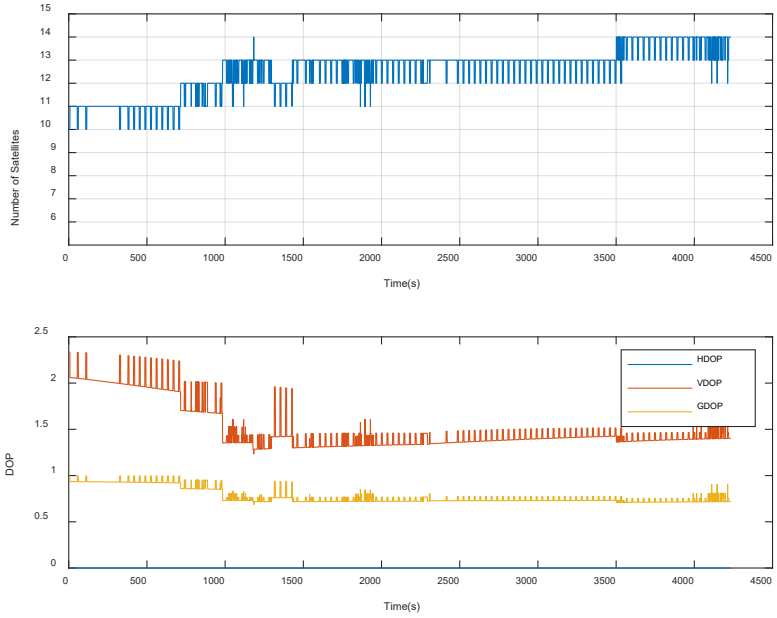

Figure 6-9 Number of SV used to generate the PVT solution and the DOP Values

6.1.2.1.2 TS04 – PVTI Performance Analysis (MRAIM GNSS DFMC: VAIM enabled)

Figure 6-10, shows integrity flags, the horizontal errors and the protection level generated using single high elevation satellite with the ramp error injected into the observation RINEX. It can be seen from the integrity flag plot that the GREEN flag is raised which in this case indicates that the following condition was met PL< AL, the alert limit is set to the value of 25 m.

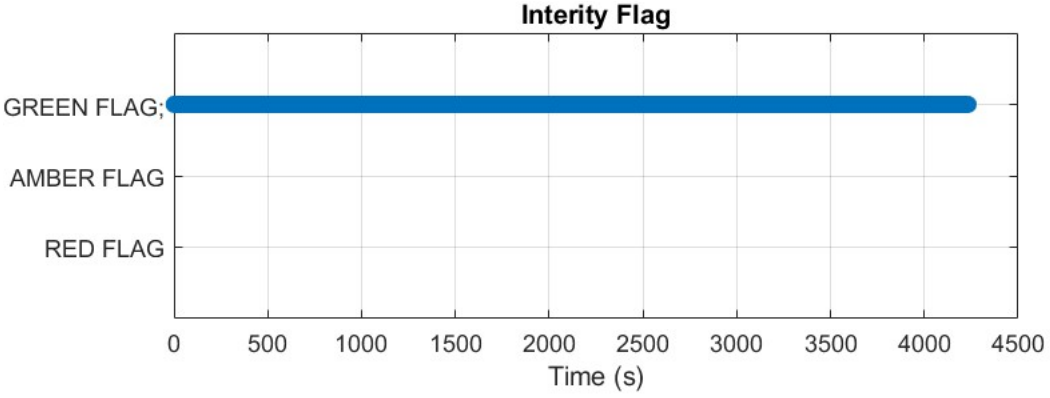

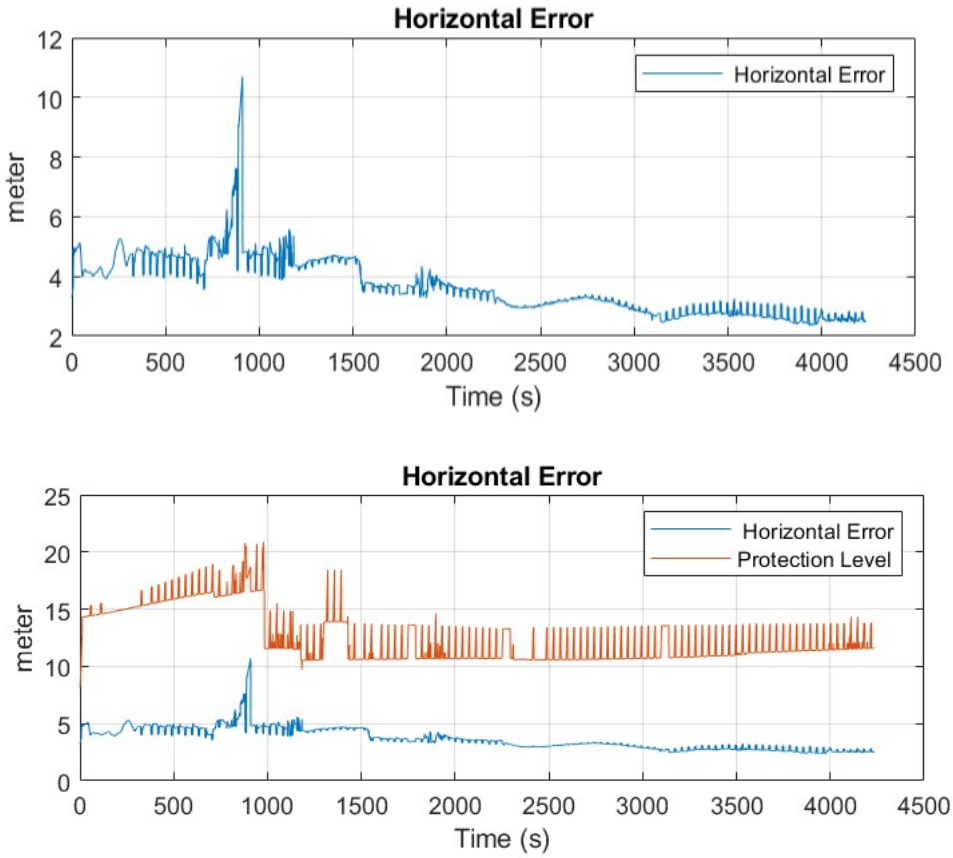

Figure 6-10 The MRAIM Integrity Flag (above), Horizontal Error(middle) and Horizontal Error vs HPL (below)

The solution performance is summarised in Table 6-9, for GNSS DFMC:

Table 6-5 TS04 –Horizontal error parameters for GNSS DFMC

	MEAN (m)	**STD(m)**	**95%(m)**
Horizontal Error: **MRAIM VAIM enabled**	3.572	0.902	5.639
Horizontal Error: **MRAIM only**	3.569	0.884	5.632

Figure 6-11 illustrate the number of satellites used to compute the PVT solution and the computed DOP.

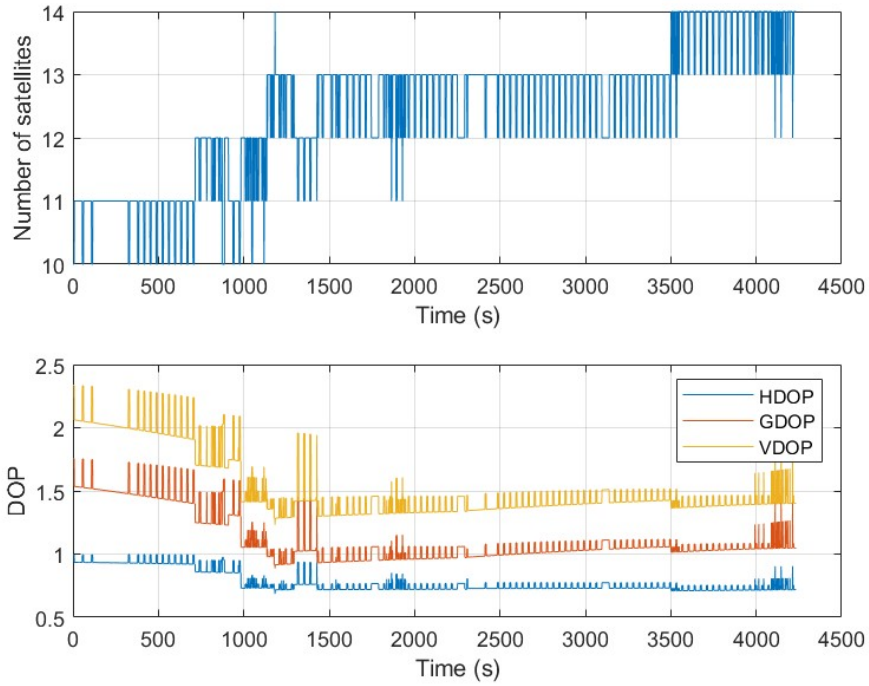

Figure 6-11 Number of SV used to generate the PVT solution and the DOP Values

6.1.2.2 Multiple High-elevation SV

This subsection shows the results generated using a smoothing constant of 100 seconds based on the following test scenario:

Test Scenario	Correction mode	Fault injection	Comment
TS.05	MGRAIM GNSS DFMC (VAIM enabled)	Multiple Satellite Clock failure (ramp) - High Elevation SV	apply ramp error on 2 high-elevation SV
TS.06	MRAIM GNSS DFMC (VAIM enabled)	Multiple Satellite Clock failure (ramp) - High Elevation SV	apply ramp error on a 2 high-elevation SV

Table 6-14 shows the configuration parameters and values used to create the ramp fault injection dataset. The ramp error at the speed of 0.4m/s is injected into the original pseudo-range of a satellite from t=844s (SOW: 202634s) for a period of 300s to end at to t = 1144s (SOW: 202934s) and a second satellite from t=2558s (SOW: 204348s) to t = 2858s (SOW: 204648s).at t=844s (SOW: 202634s) for a period of 300s to end at to t = 1144s (SOW: 202934s).

Table 6-6 TS05/TS06 Configuration

Parameter	Value	Comment
Start time [GPS Week SOW]	[2180 202634], [2180 204348]	represents the time and duration of the injection of the fault
End time [GPS Week SOW]	[2180 202934], [2180 204648]	
Constellation	['G'];	The constellation which is affected
PRN	[1], [4];	Satellites in which the fault was injected
Range drift	[0.4m/s]	

6.1.2.2.1 TS05 – PVTI Performance Analysis (MGRAIM GNSS DFMC: VAIM enabled)

Figure 6-12 and Figure 6-13 show fault detection test results from Test Scenario 05 MGRAIM. Figure 6-12 illustrates test statistics and threshold values computed for the solution generated for the dataset. The test statistics and threshold values are used within Fault Detection Test. It can be seen from the graph the point at which the test statistic exceeds the detection threshold at the point where the ramp error was injected into the file, when this occurs the “red light” integrity alarm/flag is raised. Figure 6-13, shows integrity flags and the horizontal errors within the solution generated.

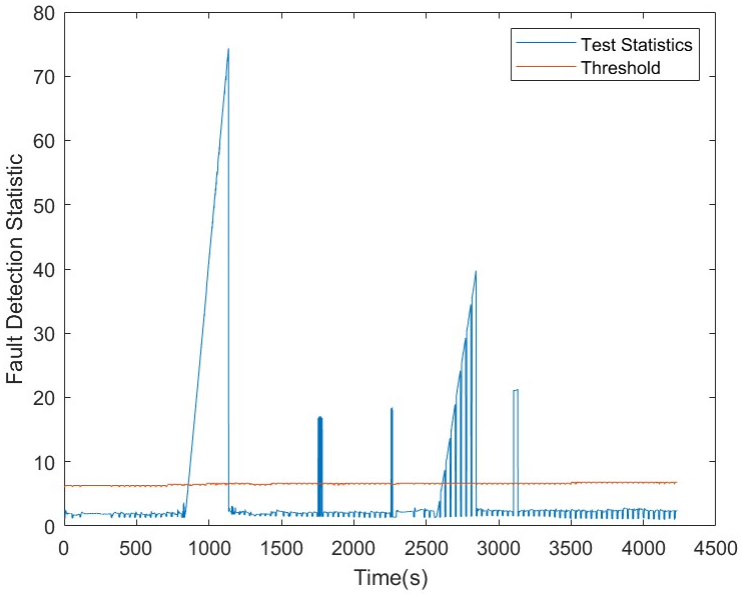

Figure 6-12 FD results from MGRAIM in Ramp fault case

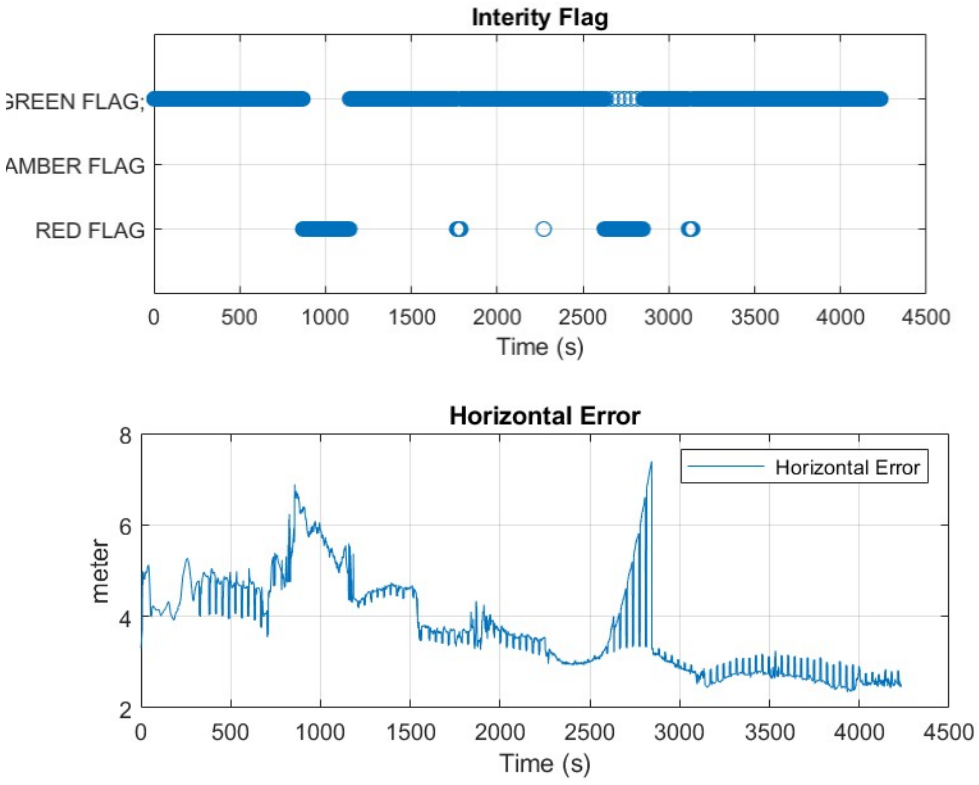

Figure 6-13 The MGRAIM Integrity Flag (above), Horizontal Error(middle) (below)

The solution performance is summarised in Table 6-15, for GNSS DFMC:

Table 6-7 TS05 - Horizontal error parameters for GNSS DFMC

	MEAN (m)	STD(m)	95%(m)
Horizontal Error: VAIM enabled	4.910	4.154	14.691
Horizontal Error: MGRAIM only	4.723	3.877	13.470

Figure 6-14 illustrate the number of satellites used to compute the PVT solution and the computed DOP.

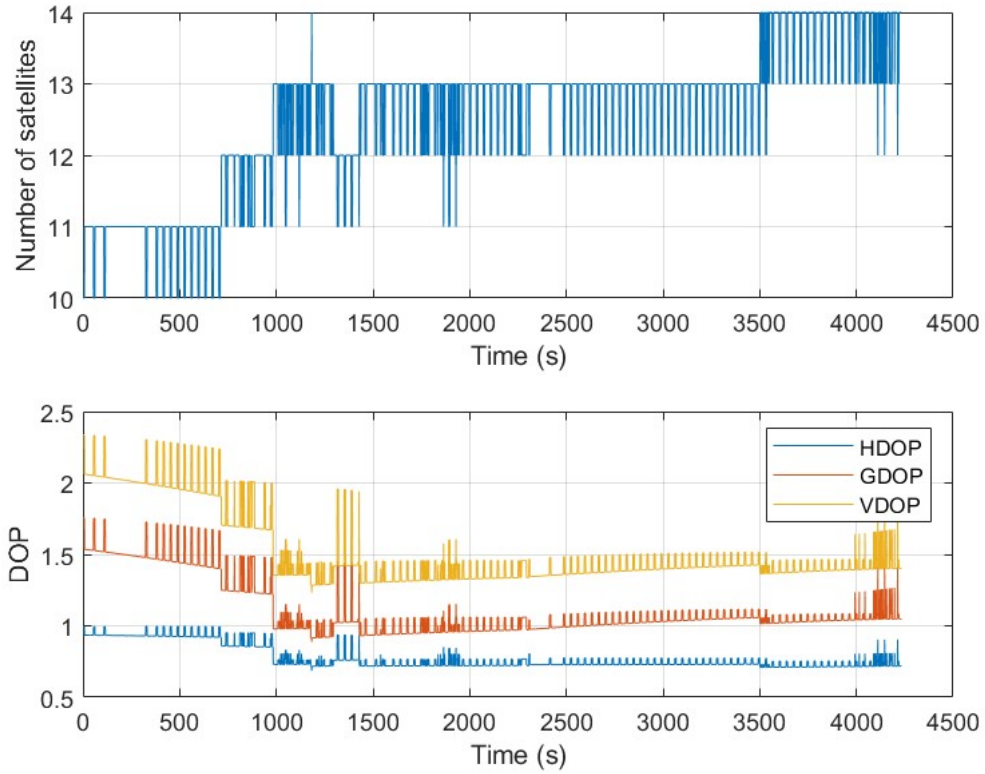

Figure 6-14 Number of SV used to generate the PVT solution and the DOP Values

6.1.2.2.2 TS06 – PVTI Performance Analysis (MRAIM GNSS DFMC: VAIM enabled)

Figure 6-15, shows integrity flags, the horizontal errors and the protection level generated using single high elevation satellite with the ramp error injected into the observation RINEX. It can be seen from the integrity flag plot that the GREEN flag is raised which in this case indicates that the following condition was met PL< AL, the alert limit is set to the value of 25 m.

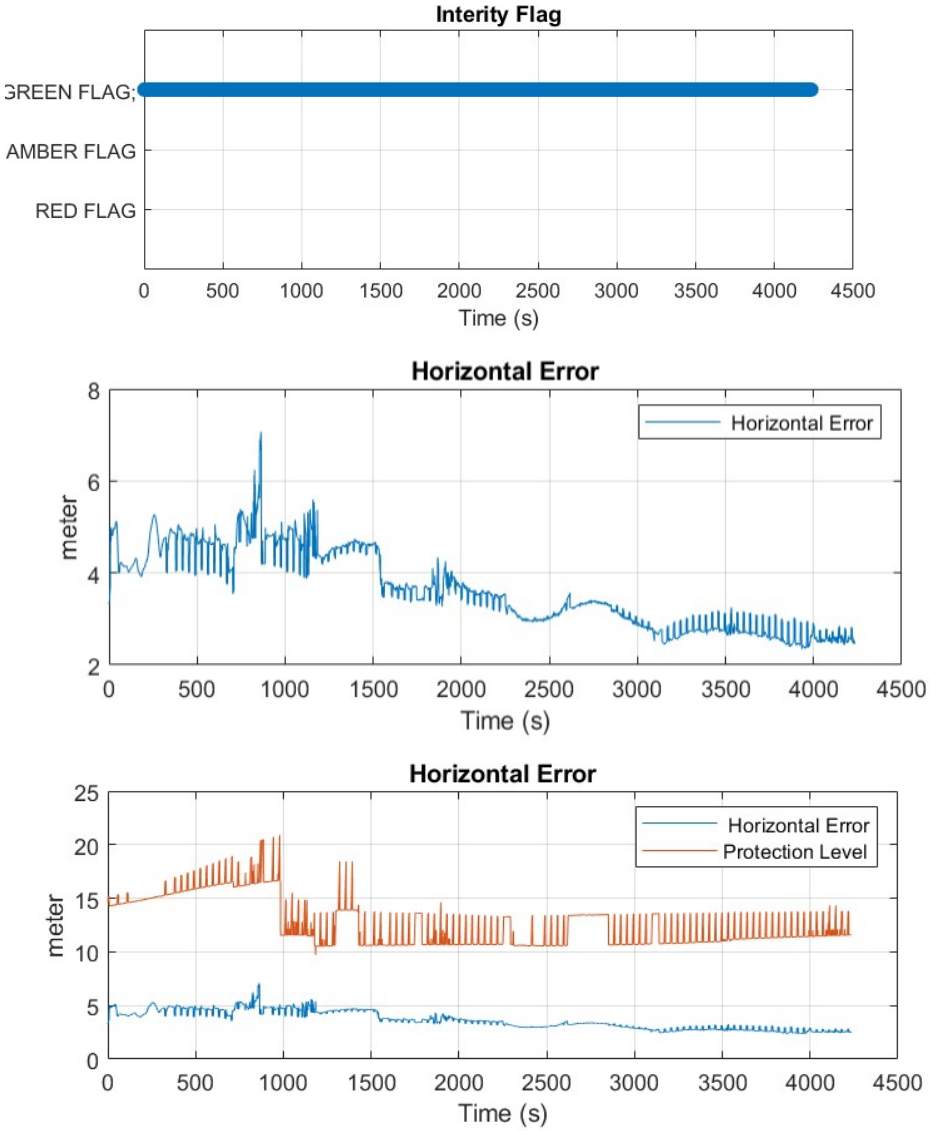

Figure 6-15 The MRAIM Integrity Flag (above), Horizontal Error(middle) and Horizontal Error vs HPL (below)

The solution performance is summarised in Table 6-16, for GNSS DFMC:

Table 6-8 TS06 –Horizontal error parameters for GNSS DFMC

	MEAN (m)	STD(m)	95%(m)
Horizontal Error: VAIM enabled	3.655	0.875	5.732
Horizontal Error: MRAIM only	3.655	0.875	5.732

Figure 6-16 illustrate the number of satellites used to compute the PVT solution and the computed DOP.

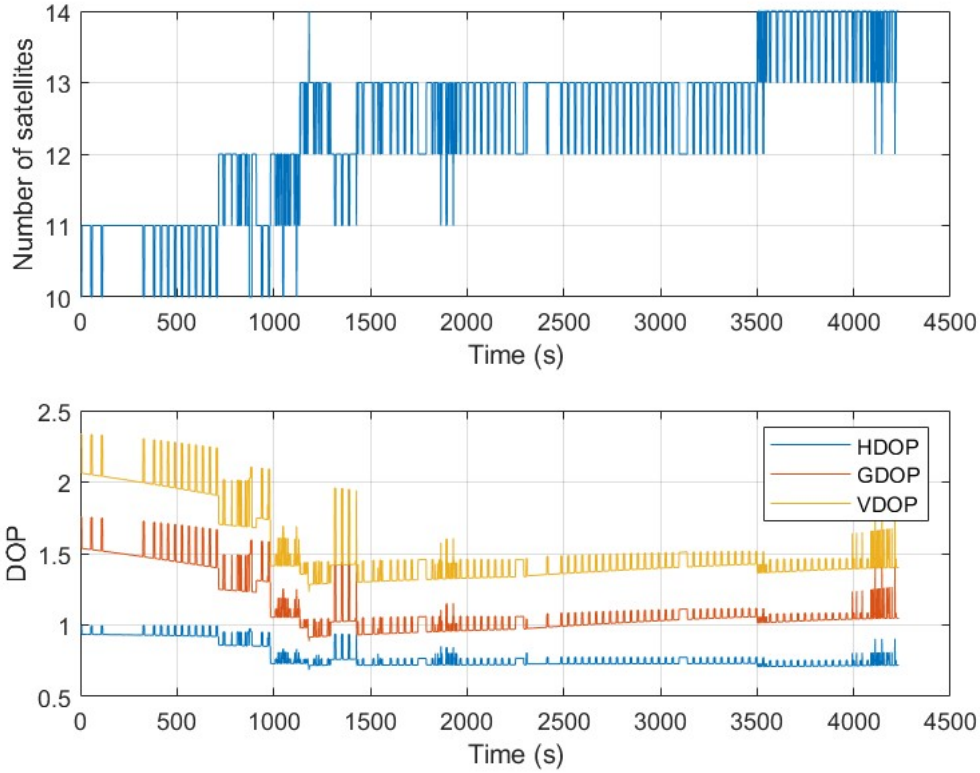

Figure 6-16 Number of SV used to generate the PVT solution and the DOP Values

6.1.3 Evaluation of GNSS Data with injected Bias Error

6.1.3.1 Single High-elevation SV

The bias fault is a basic class of GNSS anomaly, which is usually caused by the phase jump of satellite clocks or another additive fault like signal multipath. It may lead to a substantial, virtually instant shift in the user's position even by hundreds of meters.

This subsection shows the results generated using a smoothing constant of 100 seconds based on the following test scenario:

Test Scenario	*Correction mode*	*Fault injection*	*Comment*
TS.07	MGRAIM GNSS DFMC (VAIM enabled)	Single Satellite Clock failure (bias) - High Elevation SV	Applying a bias error on a single high-elevation SV
TS.08	MRAIM GNSS DFMC (VAIM enabled)	Single Satellite Clock failure (bias) - High Elevation SV	apply bias error on a single high-elevation SV

The subsection will look at the results generated using the minimum and a large detectable bias error that will raise a RED integrity flag. Table 6-19 shows the configuration parameters and values used to create the bias fault injection dataset. A fault bias of 100m was injected at times t=844s in a high-elevation satellite G01.

Table 6-9 TS07/TS08 Configuration MGRAIM DFMC case

Parameter	*Value*	*Comment*
Start time [SOW]	[2180 202634],[2180 204348]	represents the time and duration of the injection of the fault
End time [SOW]	[2180 202934], [2180 204648]	
Constellation	['G'];	The constellation on which is affected
PRN	[1];	Satellites in which the fault was injected
Range bias	[100];	fault bias values injected into the RINEX file.

6.1.3.1.1 TS07– PVTI Performance Analysis (MGRAIM GNSS DFMC: VAIM enabled)

Figure 6-17 and Figure 6-18 show fault detection test results from Test Scenario 07 MGRAIM GNSS DFMC. Figure 6-17 illustrates test statistics and threshold values computed for the solution generated for the dataset. The test statistics and threshold values are used within Fault Detection Test. It can be seen from the graph the point at which the test statistic exceeds the detection threshold, when this occurs the "red light" integrity alarm/flag is raised. Figure 6-18, shows integrity flags and the horizontal errors within the solution generated.

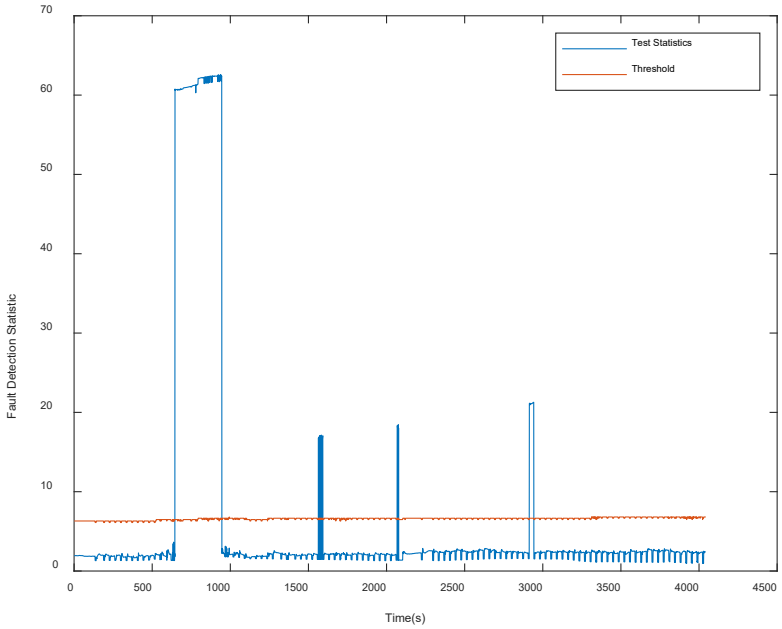

Figure 6-17 FD results from MGRAIM in Bias fault case

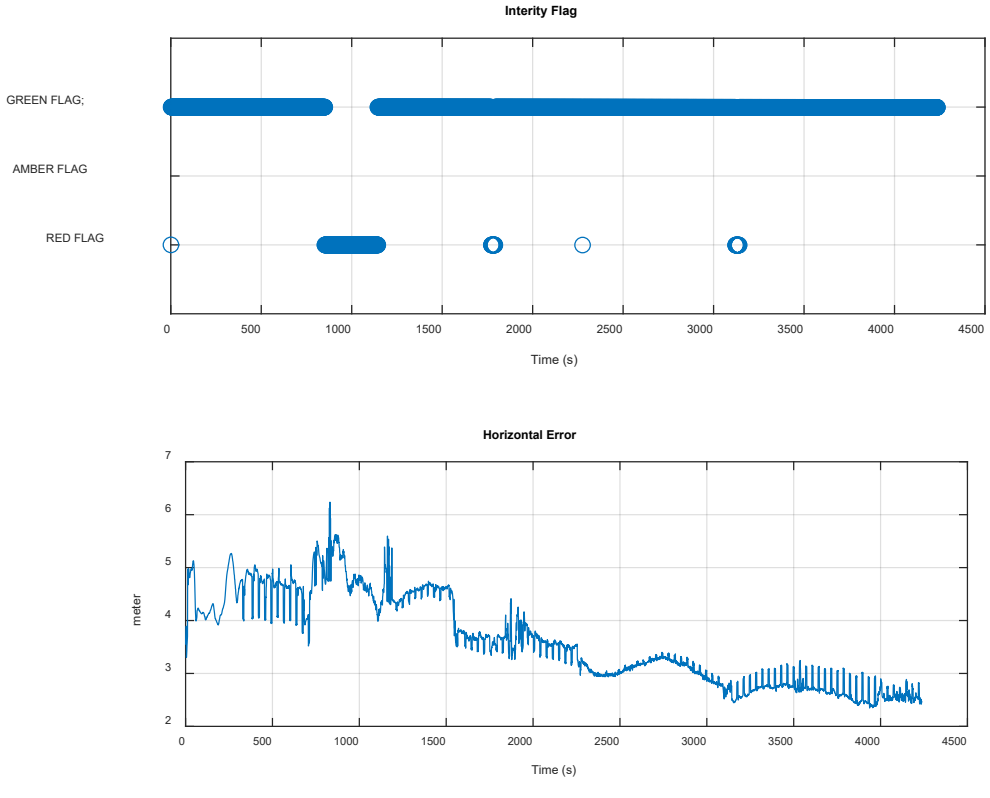

Figure 6-18 The MGRAIM Integrity Flag (above), Horizontal Error (below)

The solution performance is summarised in Table 6-20, for GNSS DFMC:

Table 6-10 TS07 - Horizontal error parameters for GNSS DFMC

	MEAN (m)	STD(m)	95%(m)
Horizontal Error: VAIM enabled	4.994	5.374	18.678
Horizontal Error: MGRAIM only	4.116	2.324	10.343

Figure 6-19 illustrate the number of satellites used to compute the PVT solution and the computed DOP.

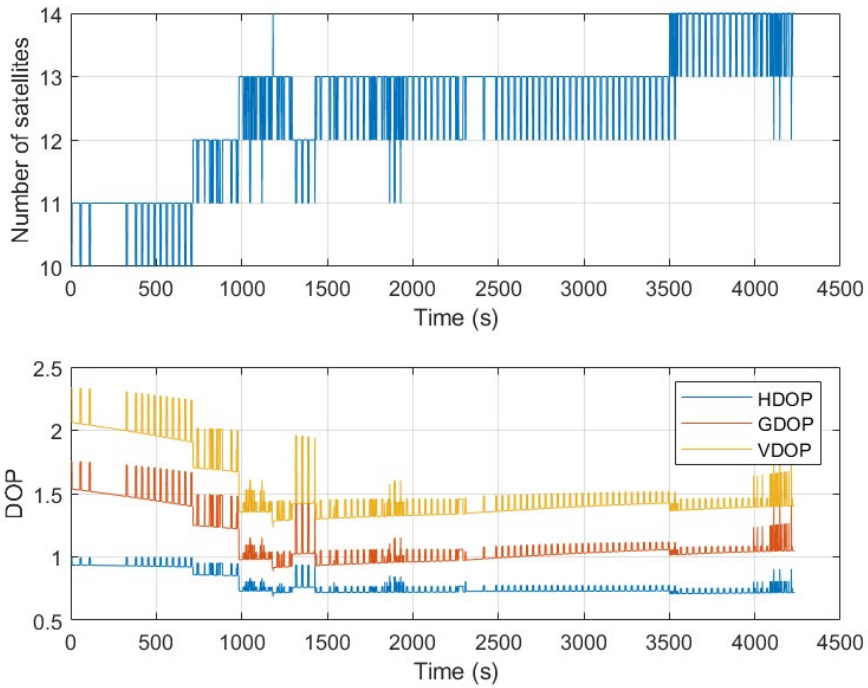

Figure 6-19 Number of SV used to generate the PVT solution and the DOP Values

6.1.3.1.2 TS08 – PVTI Performance Analysis (MRAIM GNSS DFMC: VAIM enabled)

Figure 6-20, show fault detection test results from Test Scenario 08 MRAIM GNSS DFMC, which included the integrity flags, the horizontal errors and the protection level generated. It can be seen from the integrity flag plot that the GREEN flag is raised which in this case indicates that the following condition was met PL< AL, the alert limit is set to the value of 25 m.

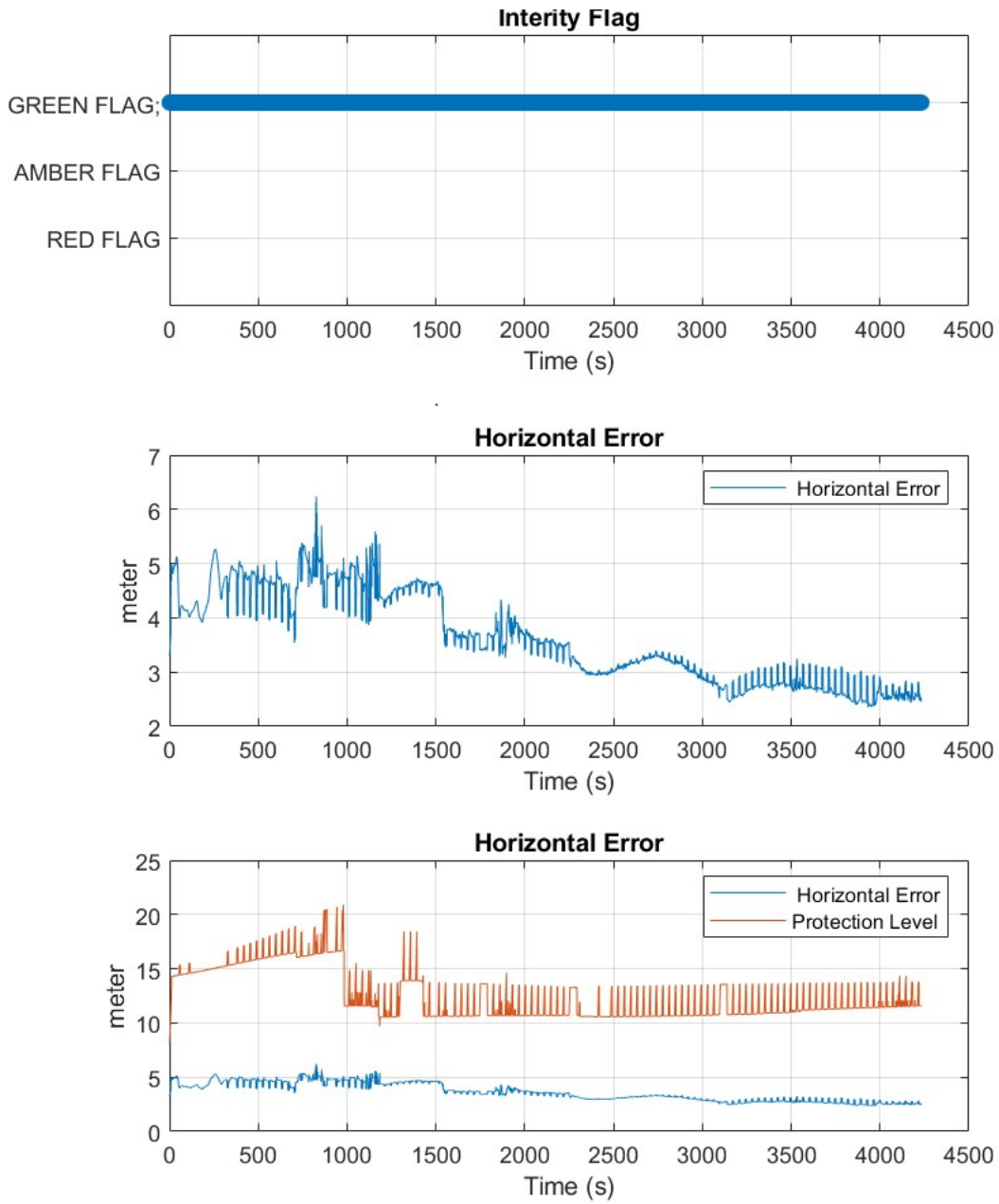

Figure 6-20 The MRAIM Integrity Flag (above), Horizontal Error (middle) and Horizontal Error vs HPL (below)

The solution performance is summarised in Table 6-21, for GNSS DFMC:

Table 6-11 TS08 - Horizontal error parameters for GNSS DFMC

	MEAN (m)	**STD(m)**	**95%(m)**
Horizontal Error: VAIM enabled	3.564	0.945	5.544
Horizontal Error: MRAIM only	3.558	0.866	5.544

Figure 6-21 illustrate the number of satellites used to compute the PVT solution and the computed DOP.

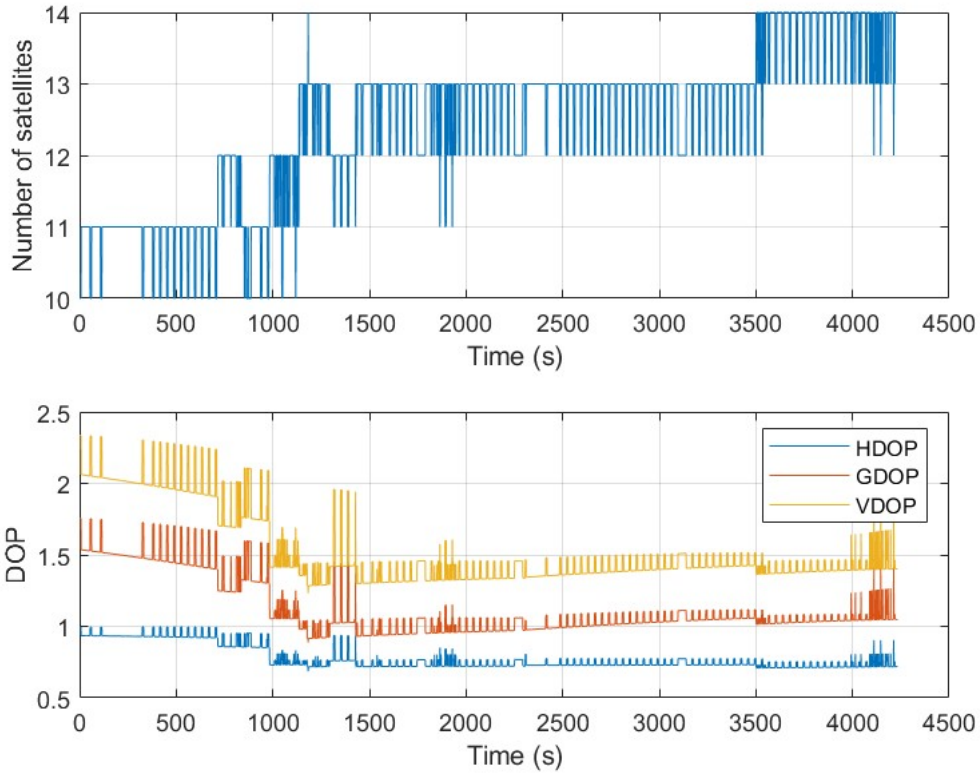

Figure 6-21 Number of SV used to generate the PVT solution and the DOP Values

6.1.3.2 Multiple High-elevation SV

This subsection shows the results generated using a smoothing constant of 100 seconds based on the following test scenario:

Test Scenario	Correction mode	Fault injection	Comment
TS.09	MGRAIM GNSS DFMC (VAIM enabled)	Multiple Satellite Clock failure (bias) - High Elevation SV	apply ramp error on 2 high-elevation SV
TS.10	MRAIM GNSS DFMC (VAIM enabled)	Multiple Satellite Clock failure (bias) - High Elevation SV	apply ramp error on a 2 high-elevation SV

Table 6-14 shows the configuration parameters and values used to create the bias fault injection dataset. A fault bias of 100m was injected into the original pseudo-range of a satellite from t=844s (SOW: 202634s) for a period of 300s to end at to t = 1144s (SOW: 202934s) and a second satellite from t=2558s (SOW: 204348s) to t = 2858s (SOW: 204648s).at t=844s (SOW: 202634s) for a period of 300s to end at to t = 1144s (SOW: 202934s).

Table 6-12 TS09/TS10 Configuration

Parameter	Value	Comment
Start time [GPS Week SOW]	[2180 202634], [2180 204348]	represents the time and duration of the injection of the fault
End time [GPS Week SOW]	[2180 202934], [2180 204648]	
Constellation	['G'];	The constellation which is affected
PRN	[1], [4];	Satellites in which the fault was injected
Range bias	[100];	

6.1.3.2.1 TS09 – PVTI Performance Analysis (MGRAIM GNSS DFMC: VAIM enabled)

Figure 6-22 and Figure 6-23 show fault detection test results from Test Scenario 09 MGRAIM. Figure 6-22 illustrates test statistics and threshold values computed for the solution generated for the dataset. The test statistics and threshold values are used within Fault Detection Test. It can be seen from the graph the point at which the test statistic exceeds the detection threshold at the point where the ramp error was injected into the file, when this occurs the “red light” integrity alarm/flag is raised. Figure 6-23, shows integrity flags and the horizontal errors within the solution generated.

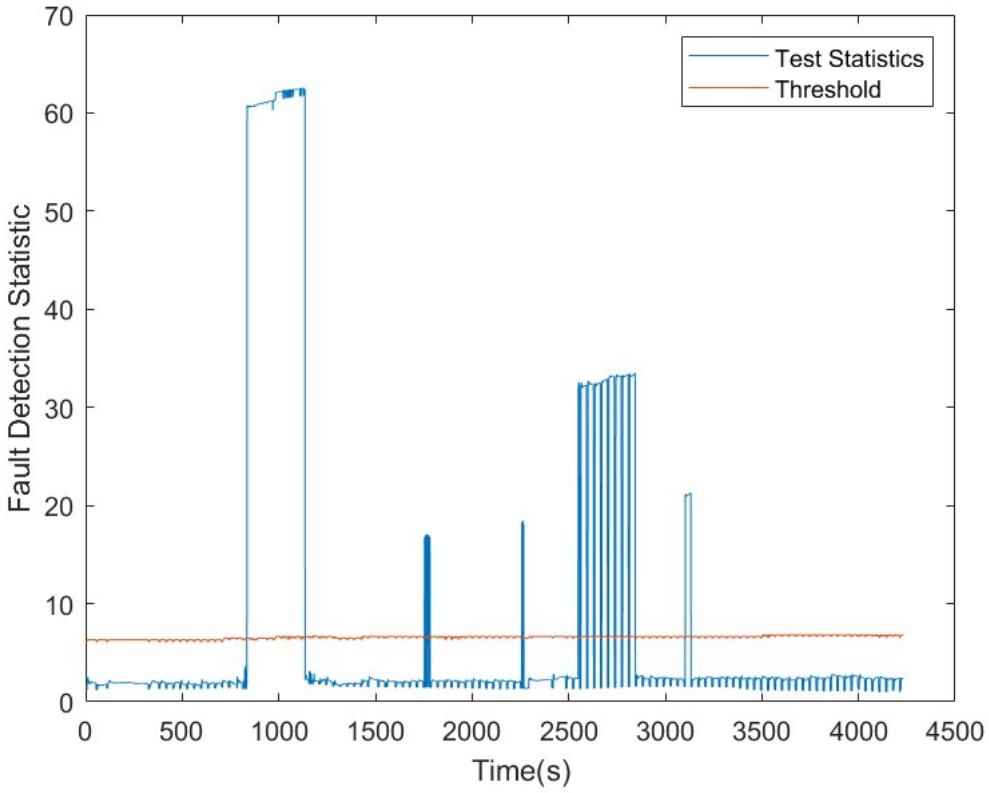

Figure 6-22 FD results from MGRAIM in Bias fault case

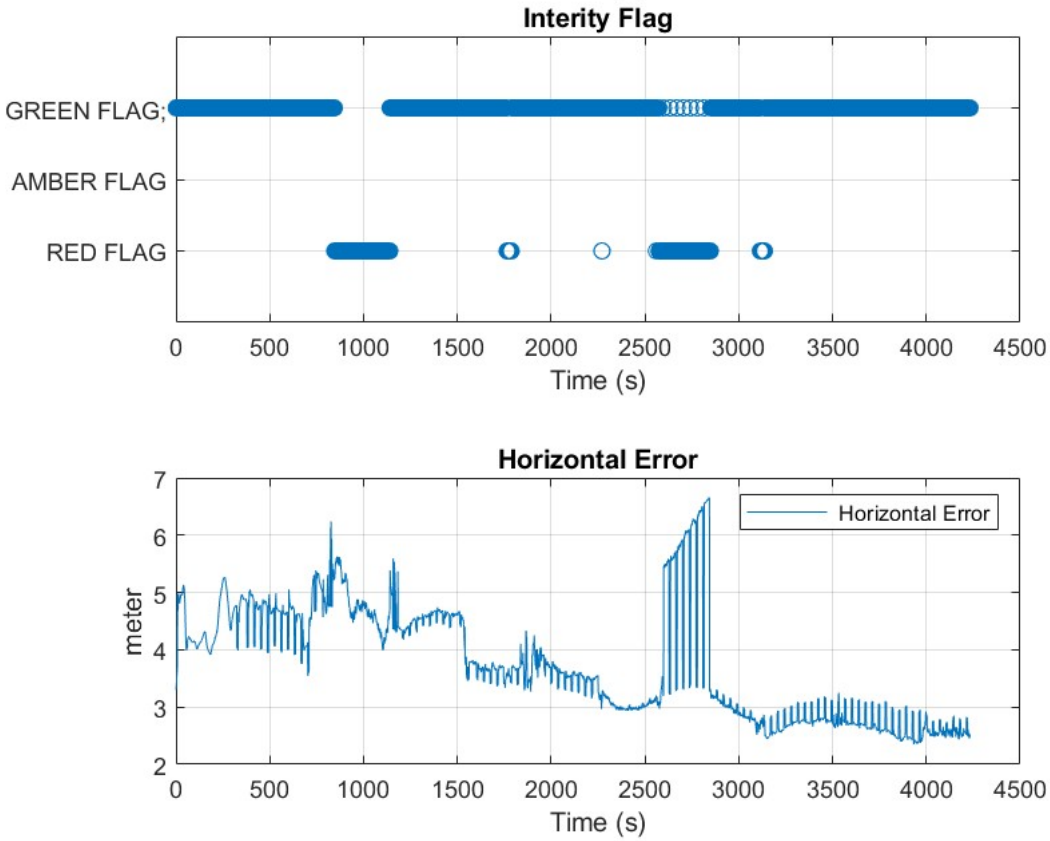

Figure 6-23 The MGRAIM Integrity Flag (above), Horizontal Error (below)

The solution performance is summarised in Table 6-27, For GNSS DFMC:

Table 6-13 TS09 - Horizontal error parameters for GNSS DFMC

	MEAN (m)	**STD(m)**	**95%(m)**
Horizontal Error: VAIM enabled	3.631	0.824	5.539
Horizontal Error: MGRAIM only	3.631	0.824	5.539

Figure 6-24illustrate the number of satellites used to compute the PVT solution and the computed DOP.

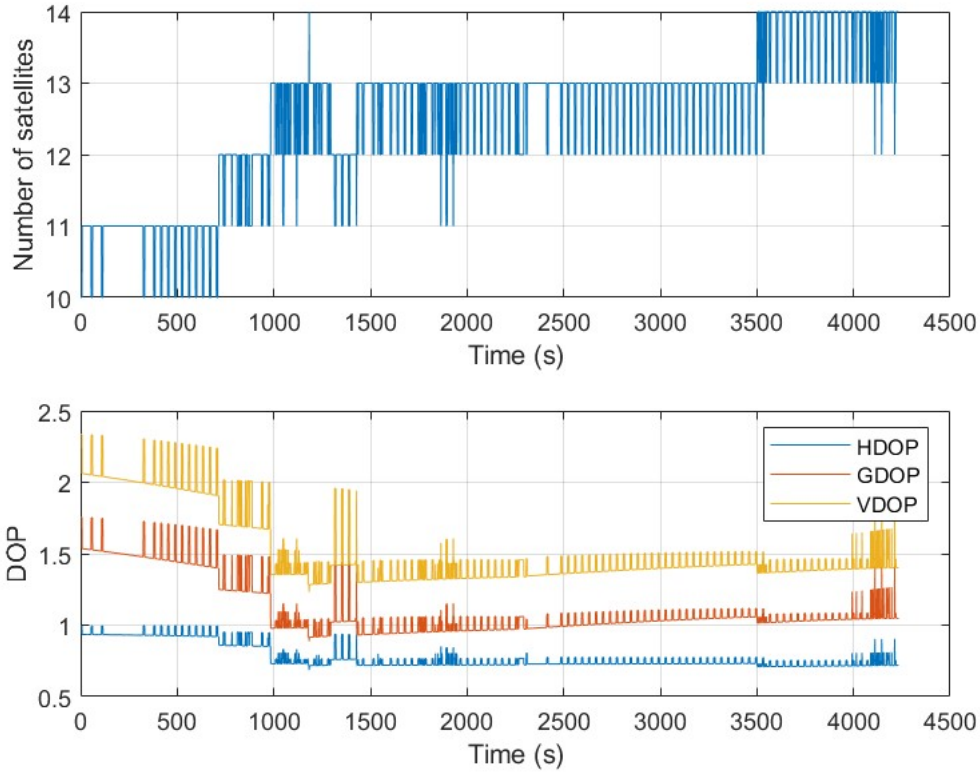

Figure 6-24 Number of SV used to generate the PVT solution and the DOP Values

6.1.3.2.2 TS10 – PVTI Performance Analysis (MRAIM GNSS DFMC: VAIM enabled)

Figure 6-25, show fault detection test results from Test Scenario 10 MRAIM GNSS DFMC, which included the integrity flags, the horizontal errors and the protection level generated. It can be seen from the integrity flag plot that the GREEN flag is raised which in this case indicates that the following condition was met PL< AL, the alert limit is set to the value of 25 m.

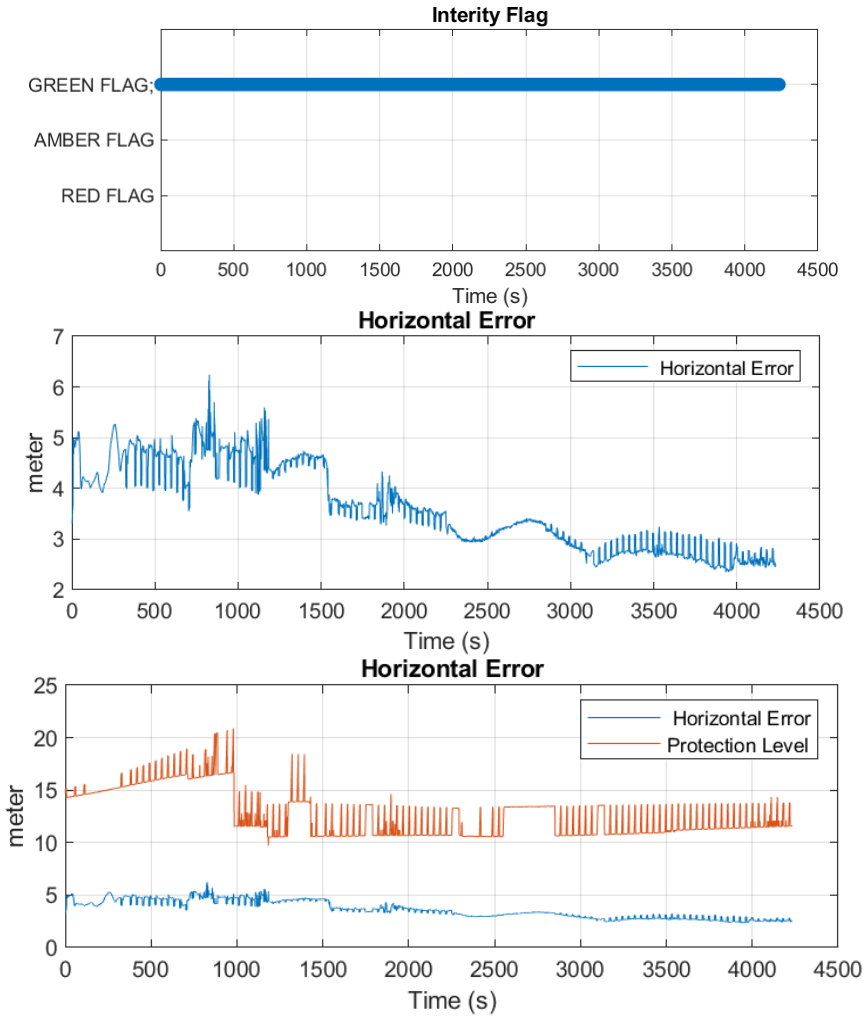

Figure 6-25 The MRAIM Integrity Flag (above), Horizontal Error (middle) and Horizontal Error vs HPL (below)

The solution performance is summarised in Table 6-28. For GNSS DFMC:

Table 6-14 TS10 - Horizontal error parameters for GNSS DFMC

	MEAN (m)	STD(m)	95%(m)
Horizontal Error: VAIM enabled	3.631	0.824	5.539
Horizontal Error: MRAIM only	3.631	0.824	5.539

Figure 6-26 illustrate the number of satellites used to compute the PVT solution and the computed DOP.

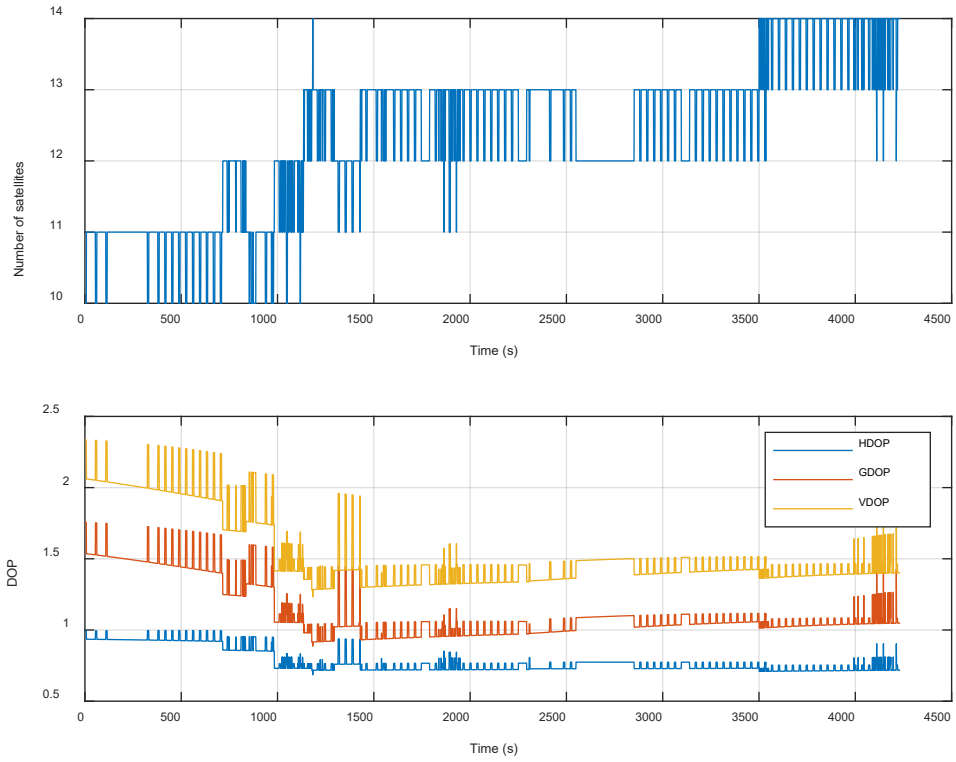

Figure 6-26 Number of SV used to generate the PVT solution and the DOP Values

6.1.4 Evaluation of GNSS Data with injected Ephemeris Error

6.1.4.1 Single high-elevation SV

The ephemeris is the satellite coordinate system. It tells the receiver where the satellite is at an instant of time. GPS receivers calculate coordinates relative to the known locations of satellites in space, a complex task that involves knowing the shapes of satellite orbits as well as their velocities, neither of which is constant. The GPS Control Segment monitors satellite locations at all times, calculates orbit eccentricities, and compiles these deviations in documents called ephemerides. An ephemeris is compiled for each satellite and broadcast with the satellite signal. There is always a certain amount of age in the ephemerides and that means that the position of the satellite expressed in its ephemeris at the moment of observation cannot be perfect. So orbital bias could be thought of as the error in the broadcast ephemeris. Even with the corrections from the GNSS ground control system, there are still small errors in the orbit that can result in up to ±2.5 metres of position error.

This subsection shows the results generated using a smoothing constant of 100 seconds based on the following test scenario:

Test Scenario	*Correction mode*	*Fault injection*	*Comment*
TS.11	MGRAIM DFMC	Single Satellite Bad Ephemeris Upload - High Elevation SV	Manually edit an ephemeris parameter within the Broadcast Navigation Message (e.g., the longitude of the ascending node (LAAN) value)
TS.12	MRAIM DFMC	Single Satellite Bad Ephemeris Upload - High Elevation SV	

Table 6-31 shows the configuration parameters and values used to create the ephemeris fault injection dataset. For this test scenario the longitude of the ascending node parameter on a high elevation was modified within the broadcast navigation message from its original value *.248039365746D+01 to .148039365746D+01*

Table 6-15 TS.11/TS.12 Configuration

Parameter	*Value*	*Comment*
Constellation	['G'];	The constellation on which is affected
PRN	[1];	Satellites in which the fault was injected
Ephemeris – The longitude of the ascending node Ω_0)	*From:0.248039365746D+01 to 0.148039365746D+01;*	The LAAN one of the orbital elements used to specify the orbit of an object in space.

6.1.4.1.1 TS11 – PVTI Performance Analysis (MGRAIM GNSS DFMC: VAIM enabled)

Figure 6-27 and Figure 6-28 show fault detection test results from Test Scenario 11 MGRAIM GNSS DFMC. Figure 6-27 illustrates test statistics and threshold values computed for the solution generated for the dataset. The test statistics and threshold values are used within Fault Detection Test. It can be seen from the graph the point at which the test statistic exceeds the detection threshold, when this occurs the “red light” integrity alarm/flag is raised. Figure 6-28, shows integrity flags and the horizontal errors within the solution generated.

The horizontal error generated from this test case are exceedingly high and not displayed here. The most significant results of this test case are that the MGRAIM algorithm was able to identify the error and raise the appropriate RED flag to indicate that the position solution is not safe for use.

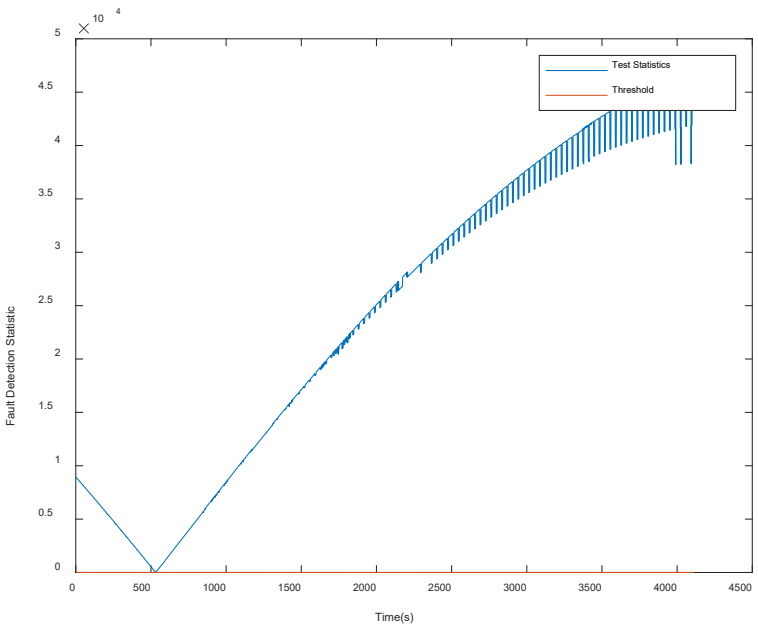

Figure 6-27 FD results from MGRAIM in Ephemeris fault case

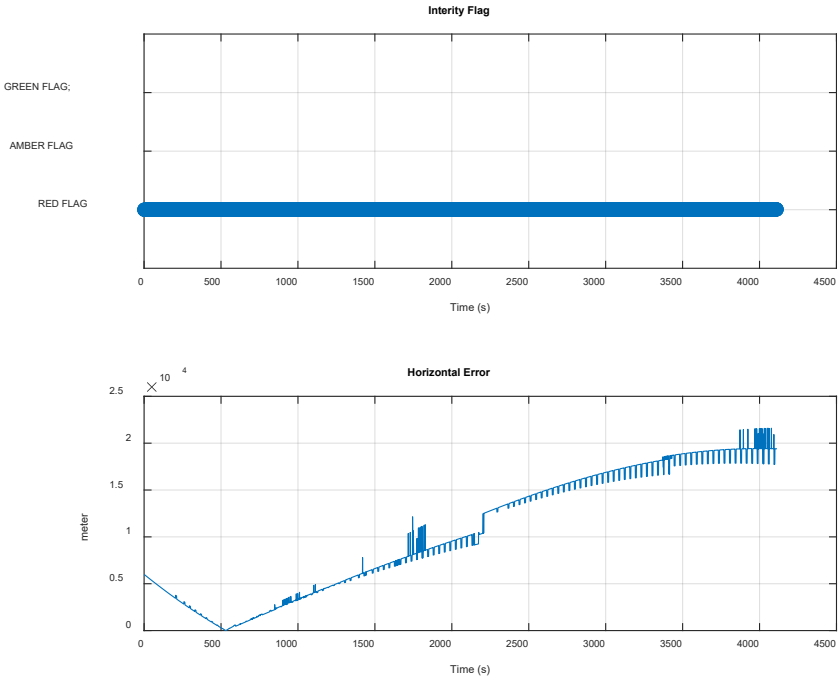

Figure 6-28 The MGRAIM Integrity Flag (above), Horizontal Error (below)

Figure 6-29 Number of SV used to generate the PVT solution and the DOP Values illustrate the number of satellites used to compute the PVT solution and the computed DOP.

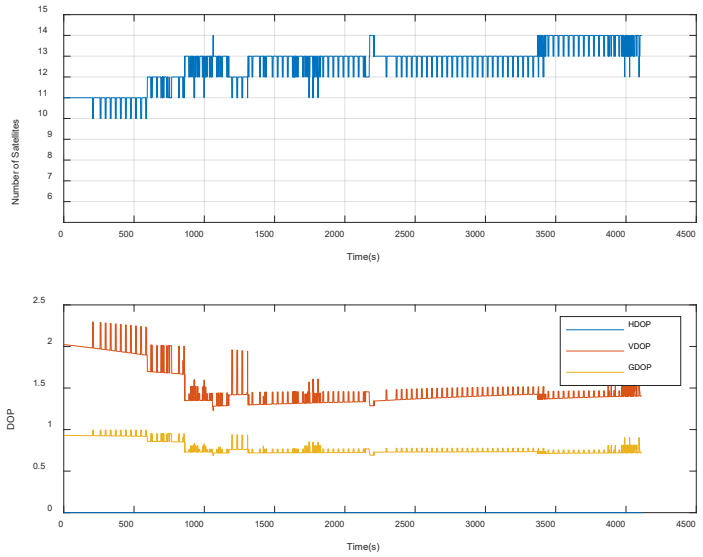

Figure 6-29 Number of SV used to generate the PVT solution and the DOP Values

6.1.4.1.2 TS12 – PVTI Performance Analysis ((MRAIM GNSS DFMC: VAIM enabled)

Figure 6-30, shows integrity flags, the horizontal errors and the protection level generated. It's been observed that the fault was detected and where possible eliminated, and the integrity RED and GREEN flags were raised accordingly. The RED flag indicates to the user at least one of the SS tests fails and the error is not excluded and/or the PL/UL is over the AL, while the GREEN flag indicates that all the tests are performed successfully and therefore the solution is ok for use. Figure 6-31, shows the number of satellites is reduced due to the exclusion of the fault satellites The Positioning error generated is significantly reduced compared to MGRAIM approach.

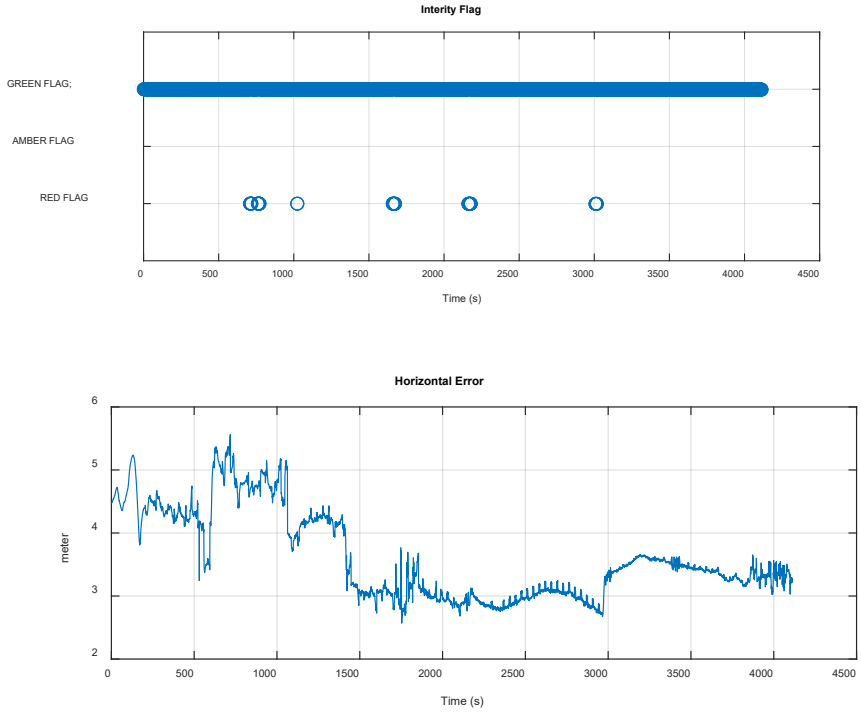

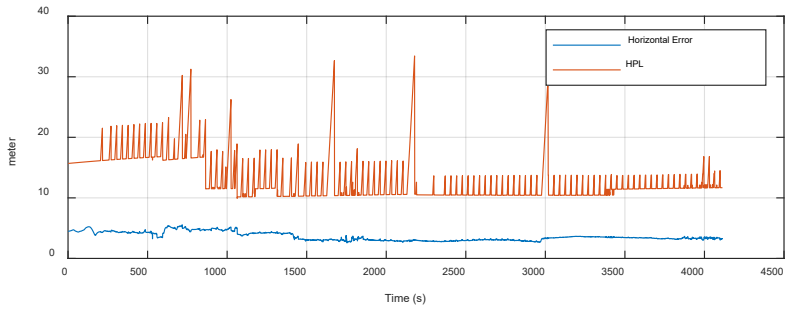

Figure 6-30 The MRAIM Integrity Flag (above), Horizontal Error (middle) and HPL (below)

The solution performance is summarised in Table 6-32 for GNSS DFMC.

Table 6-16 – TS12 - Horizontal error parameters for GNSS DFMC.

	MEAN (m)	**STD(m)**	**95%(m)**
Horizontal Error: VAIM enabled	3.65	0.70	4.96

Figure 6-31 illustrate the number of satellites used to compute the PVT solution and the computed DOP.

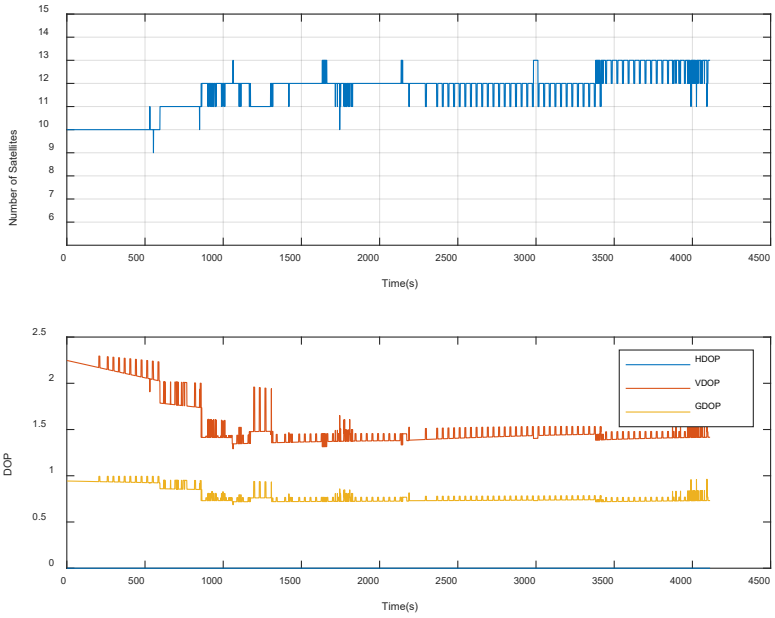

Figure 6-31 Number of SV used to generate the PVT solution and the DOP Values

6.1.4.2 Multiple High-Elevation SV

This subsection shows the results generated using a smoothing constant of 100 seconds based on the following test scenario:

Test Scenario	Correction mode	Fault injection	Comment
TS.13	MGRAIM GNSS DFMC (VAIM enabled)	Multiple Satellite Clock failure (ephemeris) - High Elevation SV	apply ramp error on 2 high-elevation SV
TS.14	MRAIM GNSS DFMC (VAIM enabled)	Multiple Satellite Clock failure (ephemeris) - High Elevation SV	apply ramp error on a 2 high-elevation SV

Table 6-14 shows the configuration parameters and values used to create the ephemeris fault injection dataset. For this test scenario the longitude of the ascending node parameter on a high elevation was modified within the broadcast navigation message from its original value *.248039365746D+01 to .148039365746D+01. T*he fault is injected into the original pseudo-range of a satellite from t=844s (SOW: 202634s) for a period of 300s to end at to t = 1144s (SOW: 202934s) and a second satellite from t=2558s (SOW: 204348s) to t = 2858s (SOW: 204648s).

Table 6-17 TS13/TS14 Configuration

Parameter	Value	Comment
Start time [GPS Week SOW]	[2180 202634],[2180 204348]	represents the time and duration of the injection of the fault
End time [GPS Week SOW]	[2180 202934], [2180 204648]	
Constellation	['G'];	The constellation which is affected
PRN	[1], [22];	Satellites in which the fault was injected
Ephemeris – The longitude of the ascending node Ω_0)	*From:0.248039365746D+01 to 0.148039365746D+01;*	The LAAN one of the orbital elements used to specify the orbit of an object in space.

6.1.4.2.1 TS013 – PVTI Performance Analysis (MGRAIM GNSS DFMC: VAIM enabled)

Figure 6-32 and Figure 6-33 show fault detection test results from Test Scenario 13 MGRAIM. Figure 6-32 illustrates test statistics and threshold values computed for the solution generated for the dataset. The test statistics and threshold values are used within Fault Detection Test. It can be seen from the graph the point at which the test statistic exceeds the detection threshold at the point where the ramp error was injected into the file, when this occurs the “red light” integrity alarm/flag is raised. Figure 6-33, shows integrity flags and the horizontal errors within the solution generated.

The horizontal error generated from this test case are exceedingly high and not displayed here. The most significant results of this test case are that the MGRAIM algorithm was able to identify the error and raise the appropriate RED flag to indicate that the position solution is not safe for use.

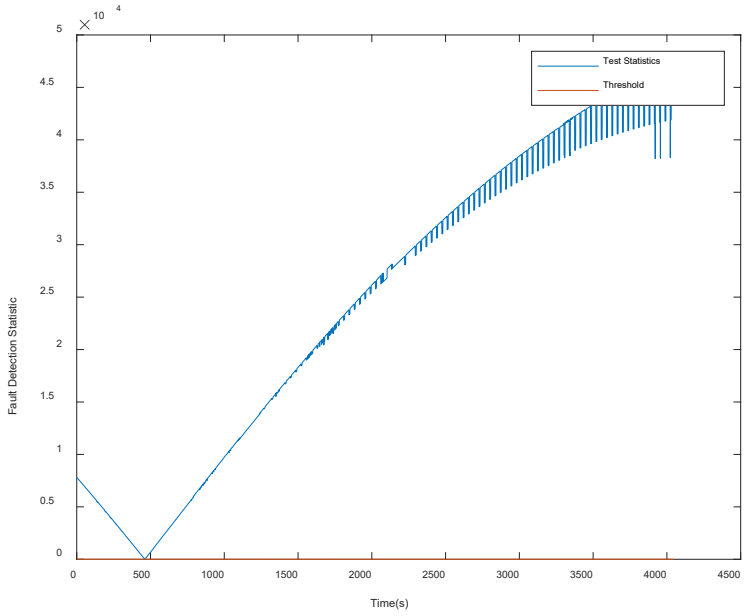

Figure 6-32 FD results from MGRAIM in Ephemeris fault case

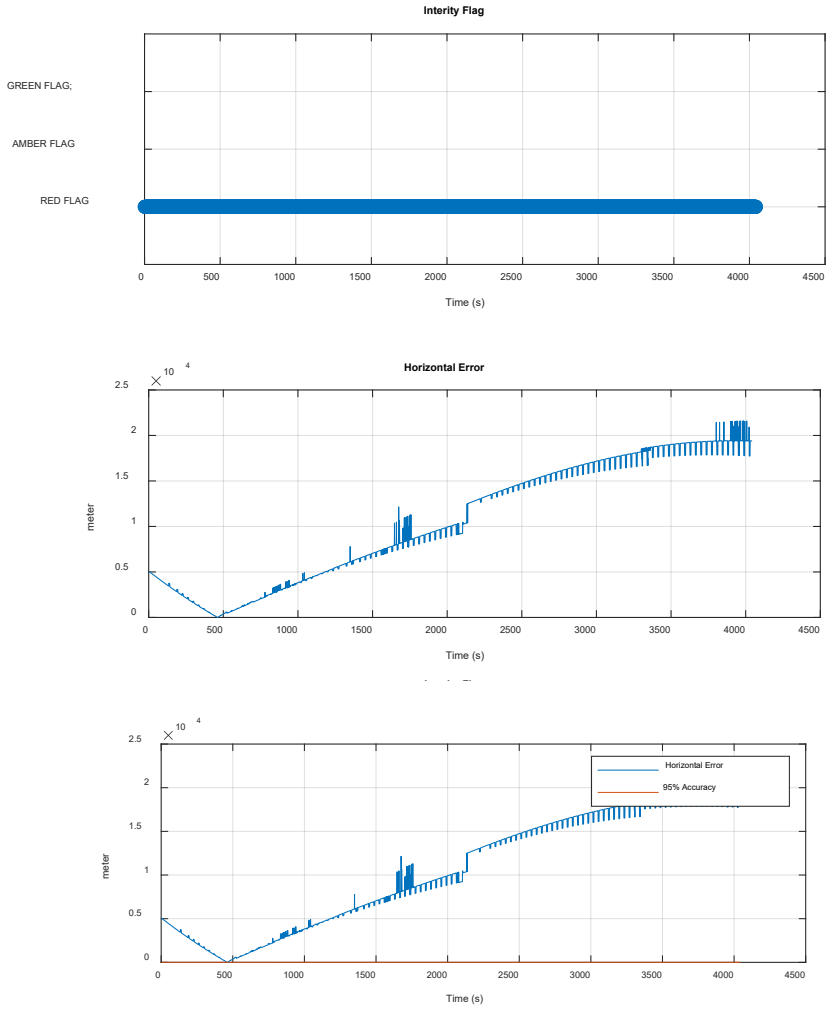

Figure 6-33 The MGRAIM Integrity Flag (above), Horizontal Error (middle) and Horizontal Error vs 95% Accuracy (below)

Figure 6-34 illustrate the number of satellites used to compute the PVT solution and the computed DOP.

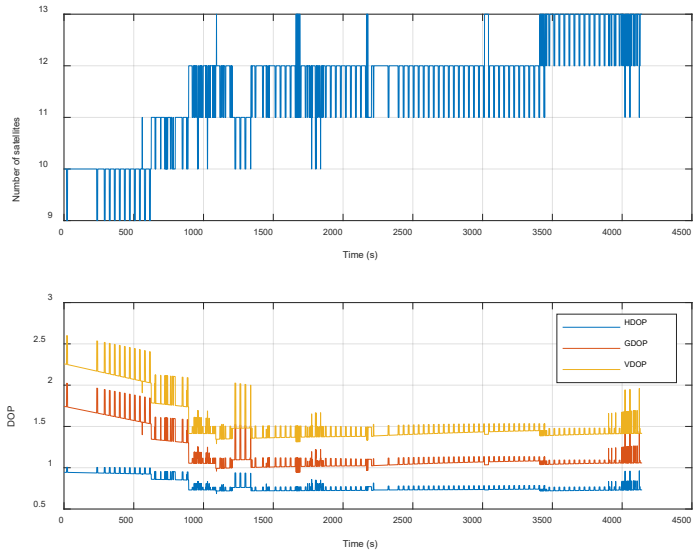

Figure 6-34 Number of SV used to generate the PVT solution and the DOP Values

6.1.4.2.2 TS14 – PVTI Performance Analysis (MRAIM GNSS DFMC: VAIM enabled)

Figure 6-35, show fault detection test results from Test Scenario 14 MRAIM GNSS DFMC, which included the integrity flags, the horizontal errors and the protection level generated. It can be seen from the integrity flag plot that the GREEN flag is raised which in this case indicates that the following condition was met PL< AL, the alert limit is set to the value of 25 m.

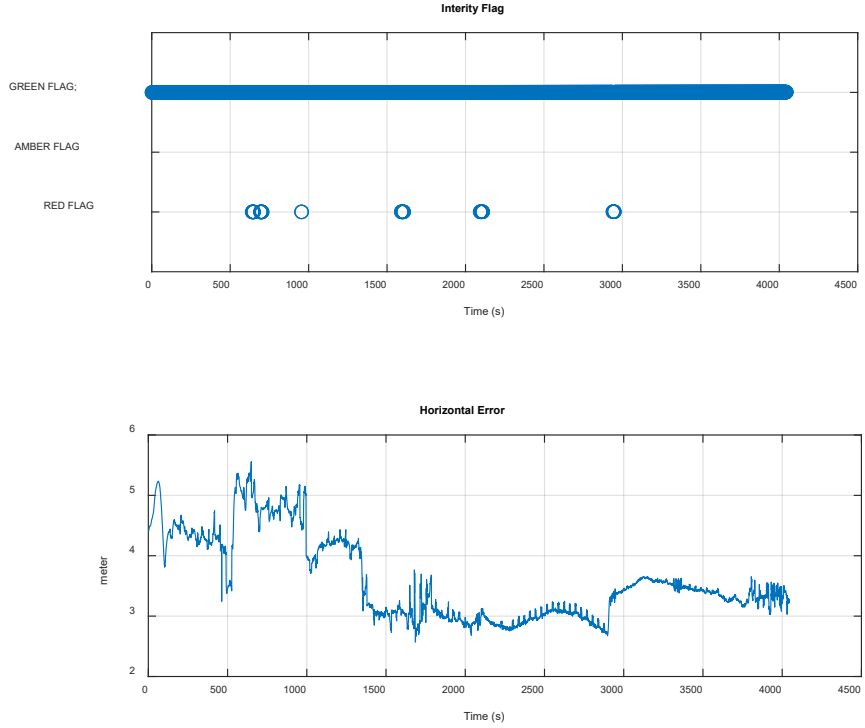

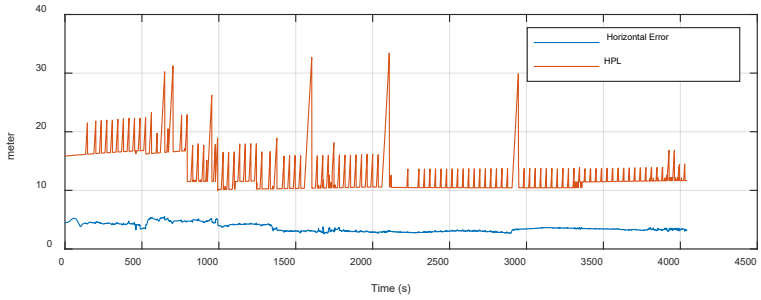

Figure 6-35 The MRAIM Integrity Flag (above), Horizontal Error (middle) and Horizontal Error vs HPL (below)

The solution performance is summarised in Table 6-36. For GNSS DFMC:

Table 6-18 TS14 - Horizontal error parameters for GNSS DFMC

	MEAN (m)	STD(m)	95%(m)
Horizontal Error: VAIM enabled	3.65	0.70	4.96

Figure 6-36 illustrate the number of satellites used to compute the PVT solution and the computed DOP.

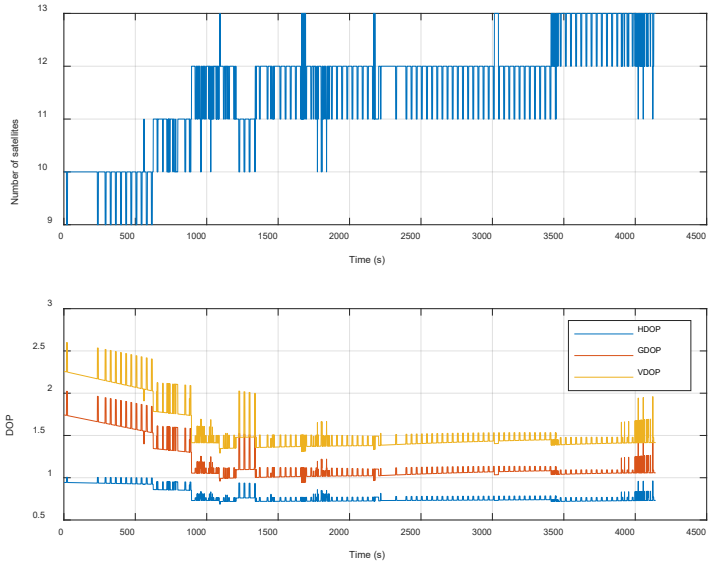

Figure 6-36 Number of SV used to generate the PVT solution and the DOP Values

6.1.5 Evaluation of GNSS Data with injected Multipath Error

6.1.5.1 Single high elevation SV

Multipath is a very localised effect, which depends only on the local environment surrounding the antenna. GNSS multipath is caused by the reception of signals arrived not only directly from satellites, but also reflected or diffracted the local objects. These signal components arrive with a certain delay, phase, and amplitude difference relative to the line-of-sight (LOS) component Multipath results in an error in pseudo range measurements and thus affects the

positioning accuracy since the multipath signal takes a longer path than the direct signal resulting in pseudorange (code phase) errors of tens of metres.

This subsection shows the results generated using a smoothing constant of 100 seconds based on the following test scenario:

Test Scenario	*Correction mode*	*Fault injection*
TS.15	MGRAIM DFMC	Applying multipath error on a single high-elevation SV
TS.16	MRAIM DFMC	Applying multipath error on a single high-elevation SV

Table 6-39 shows the configuration parameters and values used to create the multipath fault injection dataset. A fault bias of 100m was injected into the original pseudo-range of a single high elevation (G01) satellite from t=844s (SOW: 202634s) for a period of 300s to end at to t = 1144s (SOW: 202934s), with an amplitude of 5m.

Table 6-19 TS15/TS16 Configuration

Parameter	*Value*	*Comment*
Start time [SOW]	[202634]	represents the time and duration of the injection of the fault
End time [SOW]	[202934]	
Constellation	['G'];	The constellation on which is affected
PRN	[1]	Satellites in which the fault was injected
Bias	[100]	fault bias values injected into the RINEX file.
Drift	[0.4]	
Amplitude	[5]	Multipath components
Period	[30]	

6.1.5.1.1 TS15– PVTI Performance Analysis (MGRAIM GNSS DFMC: VAIM enabled)

Figure 6-37 and Figure 6-38 show fault detection test results from Test Scenario 15 MGRAIM. Figure 6-37 illustrates test statistics and threshold values computed for the solution generated for the dataset. It can be seen from the graph that the test statistic exceeds the detection threshold, when this occurs the “Red light” integrity alarm/flag is raised. It has been observed that the multipath error injected with a bias value of 100 was detected by the MGRAIM GNSS DFMC algorithm this may be attributed to the use of dual frequency multi-constellation signals. Figure 6-38, shows integrity flags and the horizontal errors within the solution generated.

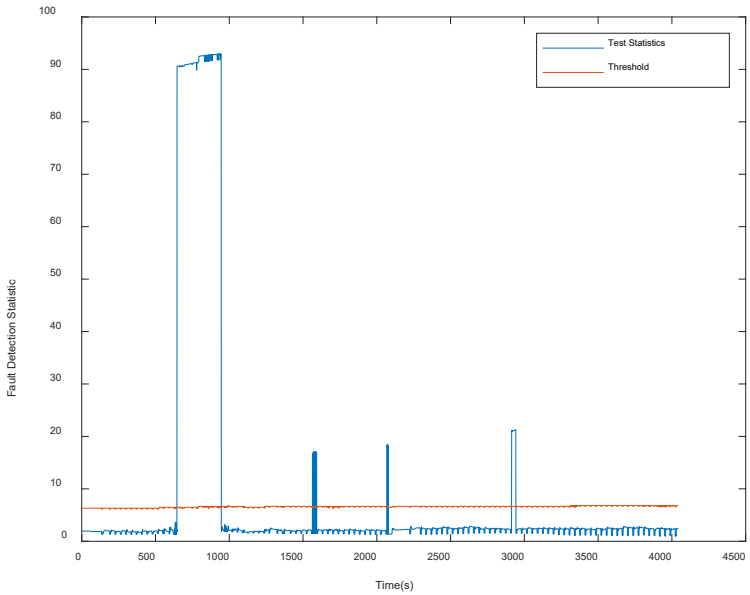

Figure 6-37 FD results from MGRAIM in Multipath fault case

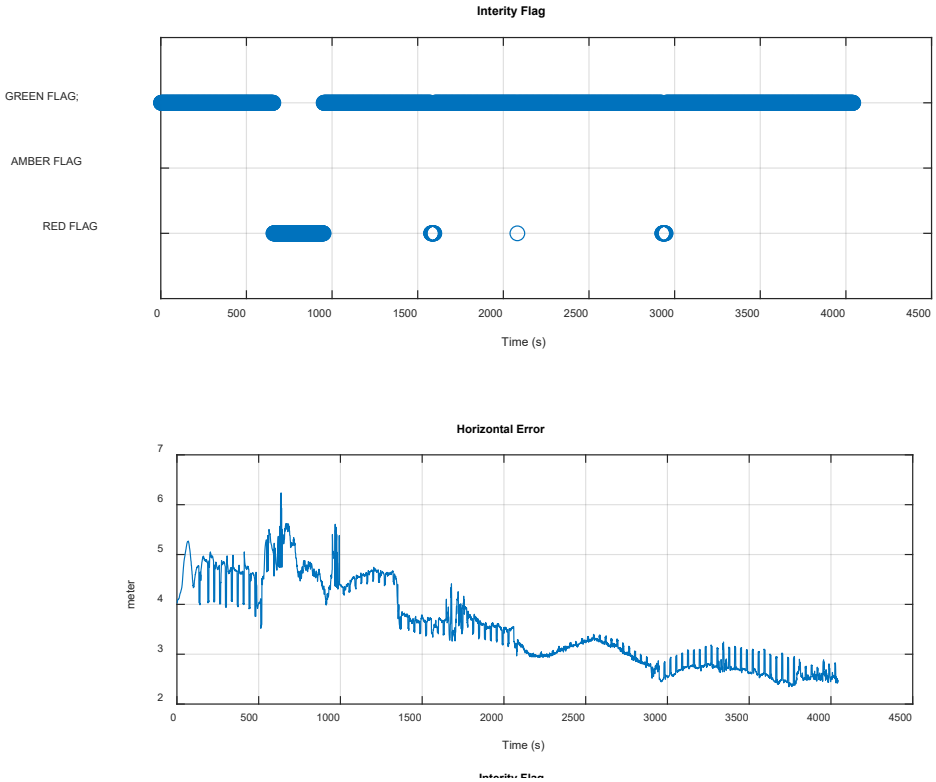

Figure 6-38 The MGRAIM Integrity Flag (above) and Horizontal Error (below)

The solution performance is summarised in Table 6-40, for GNSS DFMC.

Table 6-20 TS15 - Horizontal error parameters for GNSS DFMC

	MEAN (m)	STD(m)	95%(m)
Horizontal Error: VAIM enabled	5.788	8.286	27.576
Horizontal Error:	4.363	3.152	13.631

MGRAIM only			

Figure 6-39 illustrate the number of satellites used to compute the PVT solution and the computed DOP.

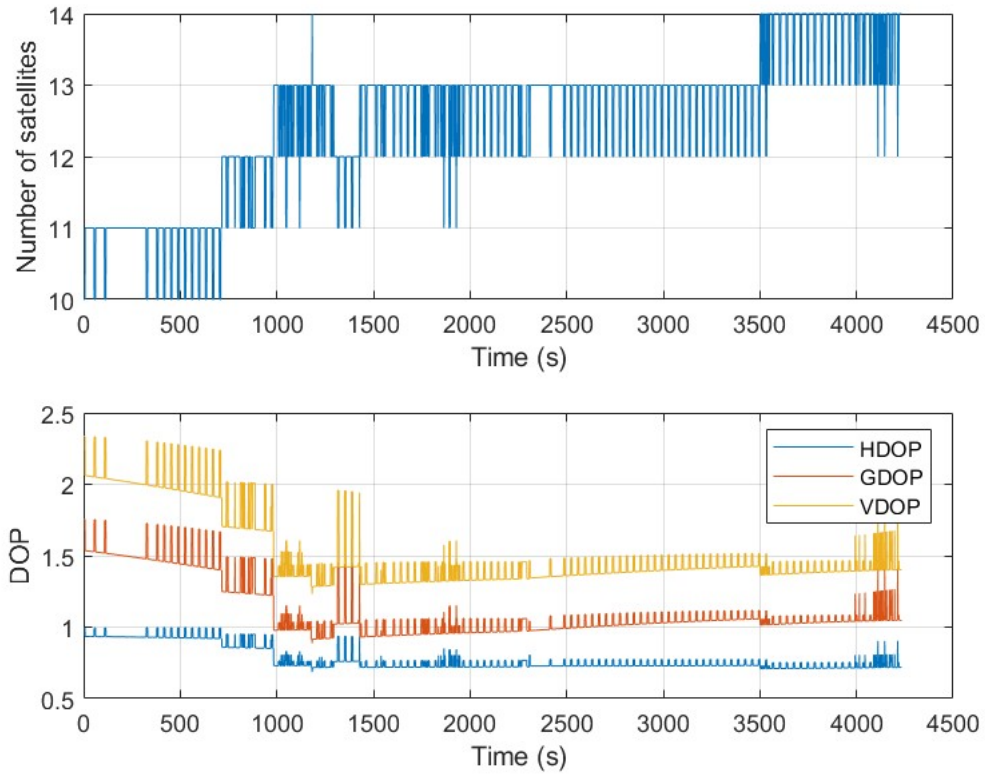

Figure 6-39 Number of SV used to generate the PVT solution and the DOP Values

6.1.5.1.2 TS16– PVTI Performance Analysis (MRAIM GNSS DFMC: VAIM enabled)

Figure 6-40 show fault detection test results from Test Scenario 16 MRAIM, which included the integrity flags, the horizontal errors and the protection level generated. It can be seen from the integrity flag plot that the GREEN flag is raised which in this case indicates that the following condition was met PL< AL, the alert limit is set to the value of 25 m, however where this condition was not met the RED flag was raised.

It has been observed that the horizontal error produced a much smaller ramp error in magnitude and duration compared to the MGRAIM result. This can be attributed to the FDE process of the MRAIM where the Solution Separation Threshold test, the function that performs a threshold test for each subset and analyses if their separation is compatible with a failure. In that case where the configured threshold was met the faulty satellite was excluded to provide a safe positioning. Figure 6-41, shows the number of satellites is reduced due to the exclusion of the fault satellites The Positioning error generated is significantly reduced compared to MGRAIM approach.

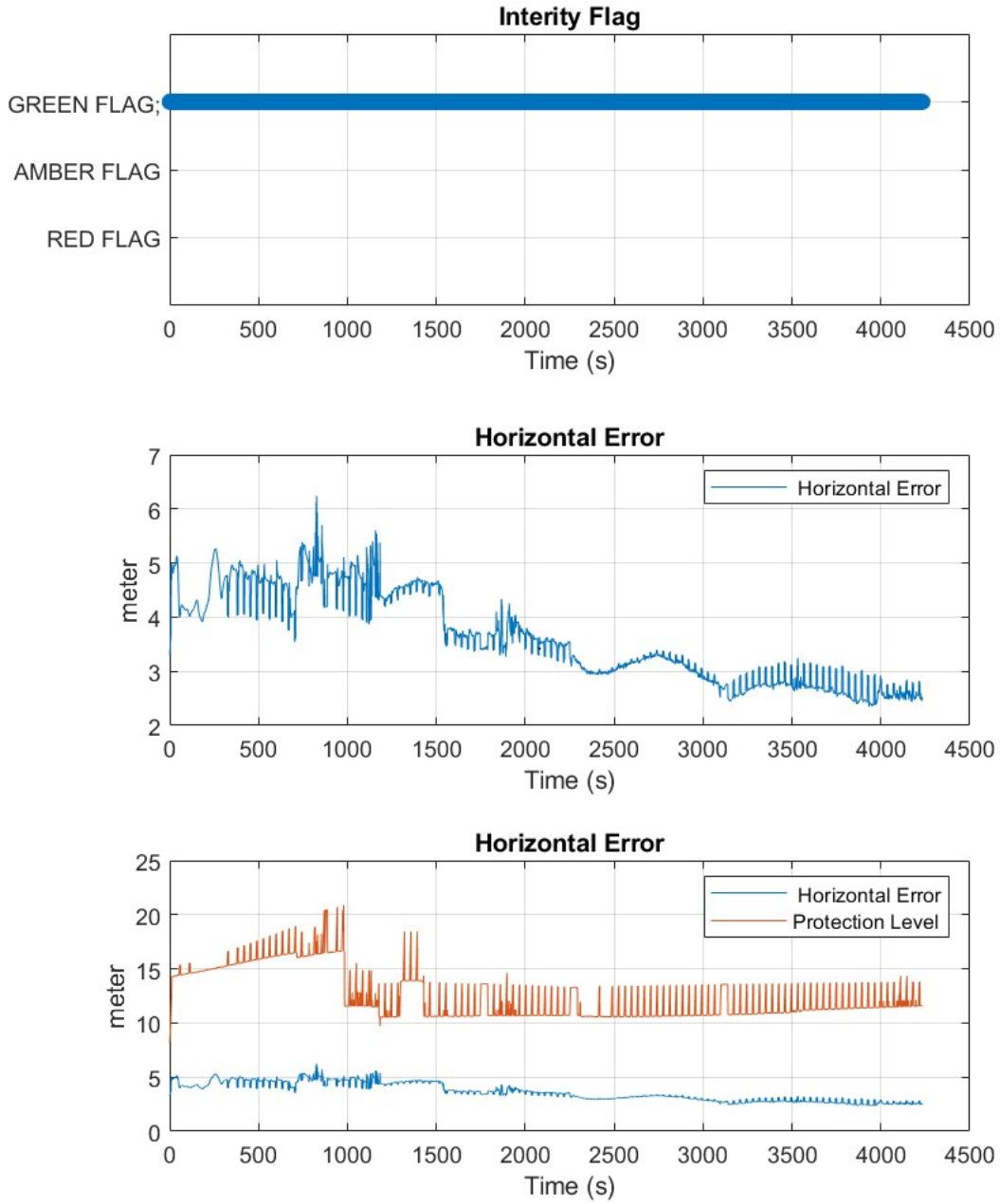

Figure 6-40 The MRAIM Integrity Flag (above) and Horizontal Error (middle) HPL (below)

The solution performance is summarised in Table 6-41 for GNSS DFMC:

Table 6-21 TS16 - Horizontal error parameters for GNSS DFMC

	MEAN (m)	**STD(m)**	**95%(m)**
Horizontal Error: VAIM enabled	3.559	0.866	5.544
Horizontal Error: MRAIM only	3.559	0.866	5.544

Figure 6-41 illustrate the number of satellites used to compute the PVT solution and the computed DOP.

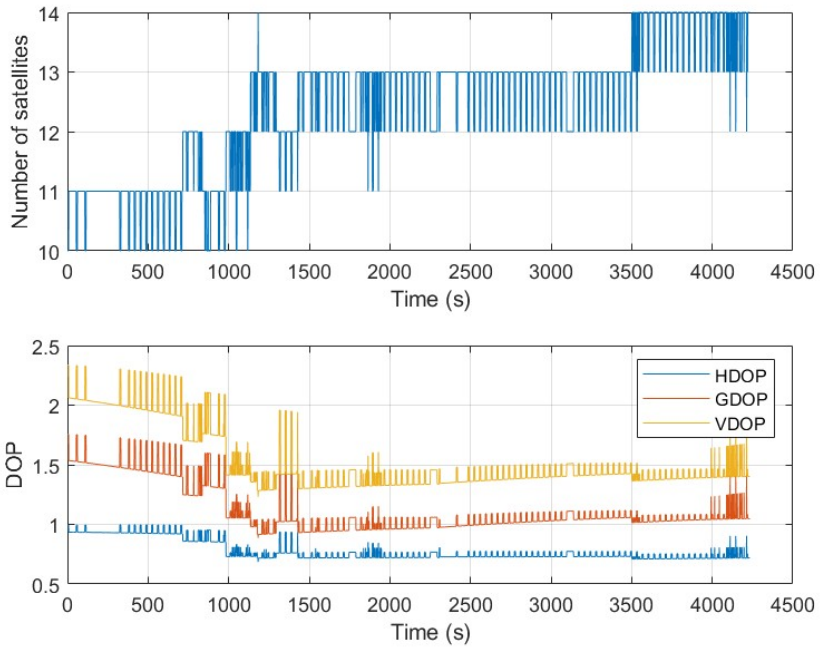

Figure 6-41 Number of SV used to generate the PVT solution and the DOP Values

6.1.5.2 Multiple High-elevation SV

This subsection shows the results generated using a smoothing constant of 100 seconds based on the following test scenario:

Test Scenario	Correction mode	Fault injection
TS.17	MGRAIM GNSS DFMC(VAIM enabled)	Applying multipath error on a Multiple GPS high-elevation SV
TS.18	MRAIM GNSS DFMC(VAIM enabled)	Applying multipath error on a Multiple GPS high-elevation SV

Table 6-22 shows the configuration parameters and values used to create the multipath fault injection dataset A fault bias of 100m was injected into the original pseudo-range of a single high elevation (G01) satellite from t=844s (SOW: 202634s) for a period of 300s to end at to t = 1144s (SOW: 202934s), a second satellite from t=2558s (SOW: 204348s) to t = 2858s (SOW: 204648s) ,both with an amplitude of 5m.

Table 6-22 TS21/TS22 Configuration

Parameter	*Value*	*Comment*
Start time [SOW]	[2180 202634],[2180 204348]	represents the time and duration of the injection of the fault
End time [SOW]	[2180 202934], [2180 204648]	
Constellation	['G', 'G'];	The constellation on which is affected
PRN	[1, 22];	Satellites in which the fault was injected
Bias	[100, 100]	fault bias values injected into the RINEX file.
Amplitude	[5, 5];	Multipath components
Period	[30, 30];	

6.1.5.2.1 TS17– PVTI Performance Analysis (MGRAIM GNSS DFMC: VAIM enabled)

Figure 6-42 and Figure 6-43 show fault detection test results from Test Scenario 17 MGRAIM. Figure 6-42 illustrates test statistics and threshold values computed for the solution generated for the dataset. The test statistics and threshold values are used within Fault Detection Test. It can be seen from the graph the point at which the test statistic exceeds the detection threshold, when this occurs the “RED” integrity flag is raised. Figure 6-43, shows integrity flags and the horizontal errors within the solution generated.

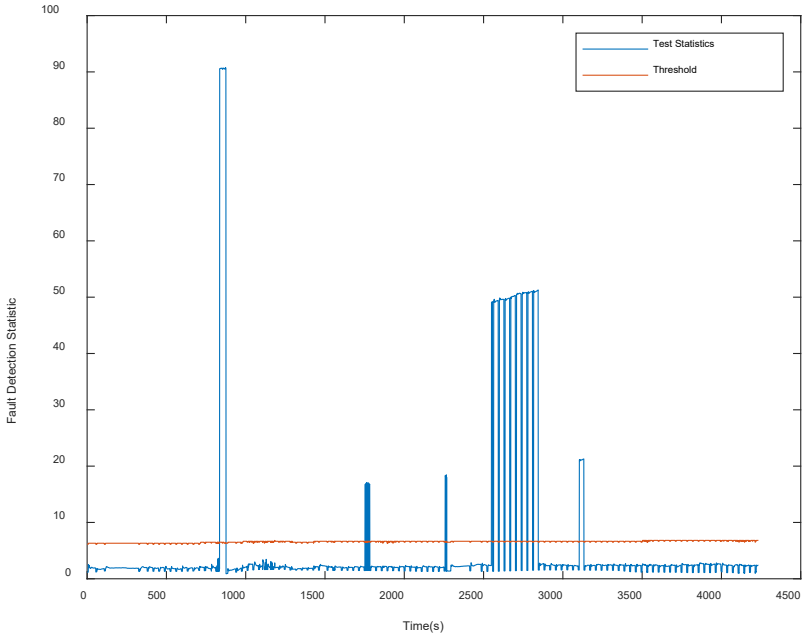

Figure 6-42 FD results from MGRAIM in Multipath fault case

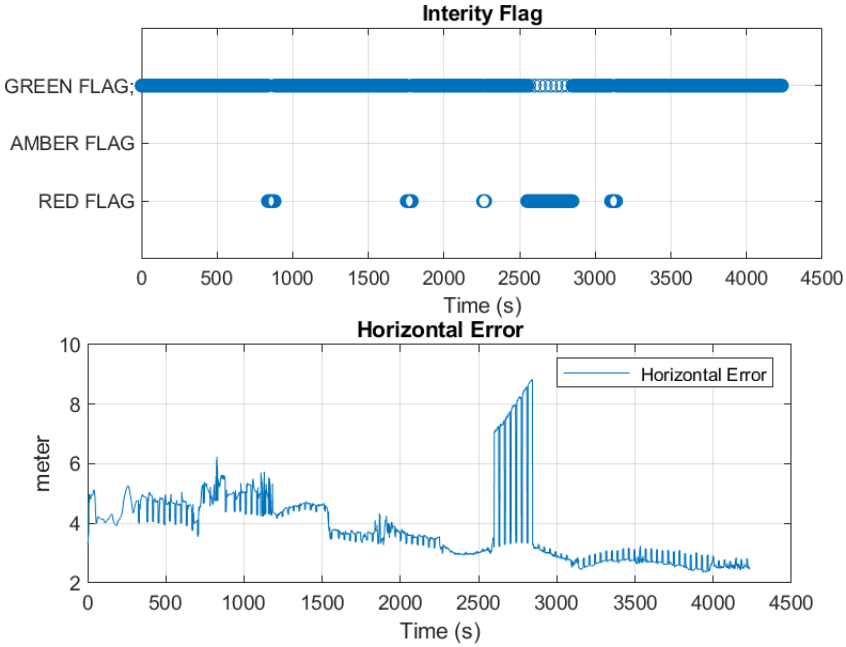

Figure 6-43 The MGRAIM Integrity Flag (above), Horizontal Error (below)

The solution performance is summarised in Table 6-23, For GNSS DFMC:

Table 6-23 TS17 - Horizontal error parameters for GNSS DFMC

	MEAN (m)	STD(m)	95%(m)
Horizontal Error: VAIM enabled	5.944	8.445	35.653
Horizontal Error: MGRAIM only	5.629	7.586	35.360

Figure 6-44 illustrate the number of satellites used to compute the PVT solution and the computed DOP.

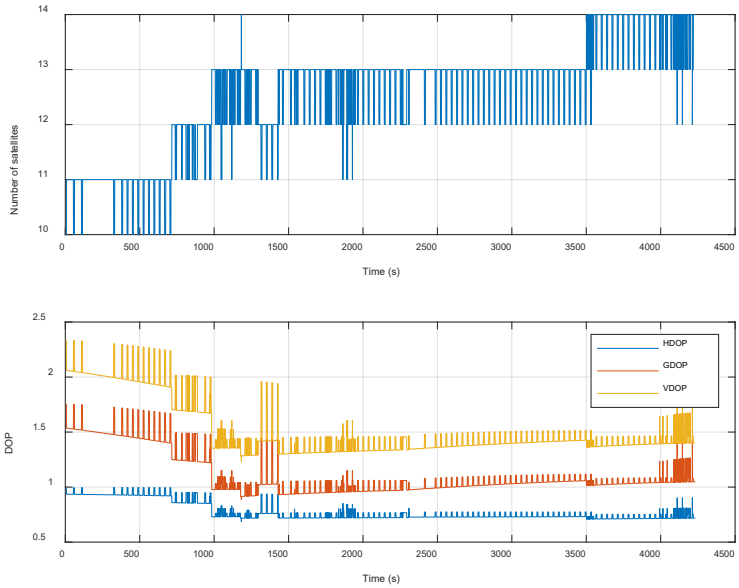

Figure 6-44 Number of SV used to generate the PVT solution and the DOP Values

6.1.5.2.2 TS18 – PVTI Performance Analysis (MRAIM GNSS DFMC: VAIM enabled)

Figure 6-35, show fault detection test results from Test Scenario 18 MRAIM GNSS DFMC, which included the integrity flags, the horizontal errors and the protection level generated. It can be seen from the integrity flag plot that the GREEN flag is raised which in this case indicates that the following condition was met PL< AL, the alert limit is set to the value of 25 m.

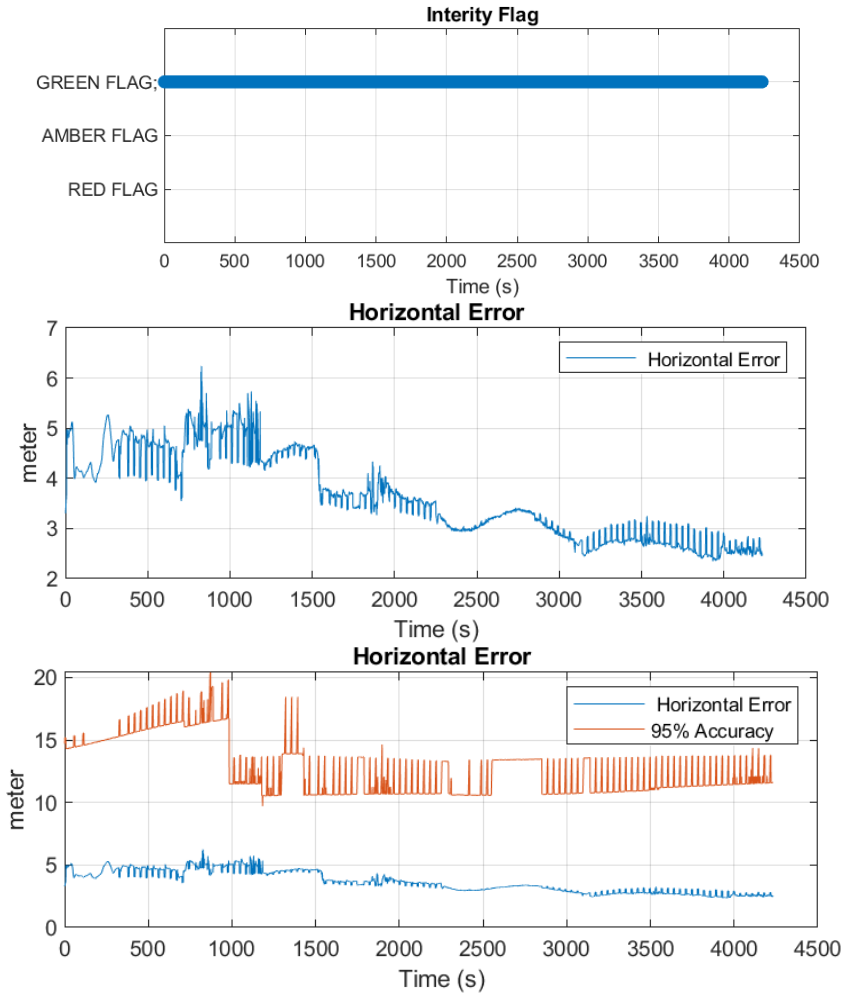

Figure 6-45 The MRAIM Integrity Flag (above), Horizontal Error (middle) and Horizontal Error vs HPL (below)

The solution performance is summarised in Table 6-24. For GNSS DFMC:

Table 6-24 TS18 - Horizontal error parameters for GNSS DFMC

	MEAN (m)	STD(m)	95%(m)
Horizontal Error: VAIM enabled	3.638	0.832	5.539
Horizontal Error: MRAIM only	3.638	0.832	5.539

Figure 6-36 illustrate the number of satellites used to compute the PVT solution and the computed DOP.

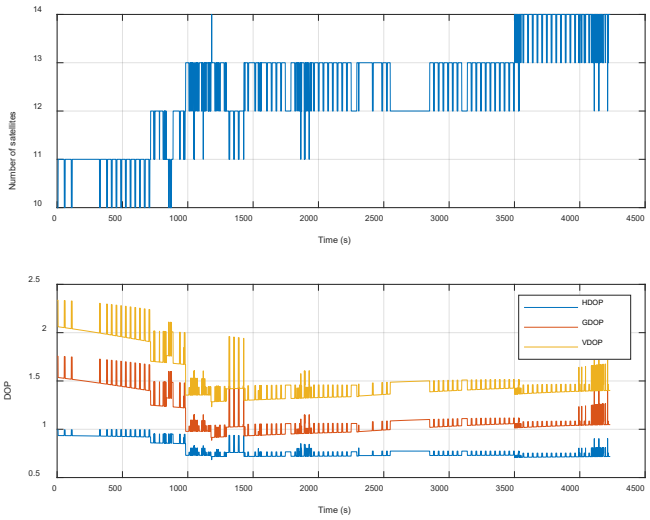

Figure 6-46 Number of SV used to generate the PVT solution and the DOP Values

6.2 Summary

The section examined the PVT solution generated using the algorithm described in Section 4, which focused Vessel Autonomous Integrity Monitoring: which is a maritime-specific implementation of the M(G)RAIM concepts developed in this project to provide the requested integrity including dead-reckoning techniques, similar to aircraft autonomous integrity monitoring (AAIM) concept used in aviation, enhancing user-level integrity and providing additional resilience in the navigation solution. Functional testing and performance evaluation were conducted based on the collection of real GNSS data (GPS and Galileo observables) in the fjord at Trondheim, Norway. Comparisons were made to the integrity algorithm developed with EGNOS GNSS DFMC enabled. To evaluate the VAIM algorithm's ability to use information from non-GNSS sensors to perform a consistency check on the positioning domain, and to perform a safe propagation technique of the last GNSS estimated epoch and its positioning accuracy of 95% (ACC95) or protection level (PL) in case of GNSS outage or significant performance degradation to improve performance on top of detecting and, where applicable, excluding faults. Simulated data was used with faults injected into the RINEX file. The simulated data provided an option to cover scenarios that would otherwise not be possible using field data alone.

The results presented within this section are for faults applied on single and multiple satellites and have shown that the algorithm is able to compute a PVT solution using the MGRAIM and MRAIM concepts with VAIM enables. It has been observed that the MGRAIM algorithm is able to detect the fault and raise the appropriate integrity status flag. While the MRAIM algorithm can detect and exclude the fault and compute the related HPL. Additionally, [RD.16] provides further results on the functional of the VAIM algorithm.

7 FEASIBILITY ASSESSMENT OF VAIM

This section assesses the feasibility of a maritime VAIM solution considering both technical and cost considerations.

As it has been demonstrated in section 6, the VAIM algorithm is clearly technically feasible, as it can improve the performance of M(G)RAIM algorithms that only use GNSS. This concept follows the IMO's approach in [RD.3] and [RD.4] for multi-system shipborne receivers, where positioning and integrity information from different sensors are fused to provide more robust, accurate, and safer positioning.

The proposed algorithm is developed for a combination of a speed sensor and compass. However, the high-level idea is technology-agnostic and could be easily adapted to any other sensor onboard a SOLAS vessel or expanded to use more than one dead reckoning sensor simultaneously. It would only be necessary to modify the propagation equations. For example, IMUs or laser sensors could be considered for further VAIM developments.

It is also important to note that VAIM is an algorithm that works on top of M(G)RAIM, so its overall performance depends on the GNSS algorithm selected. VAIM smooths out performance, backs up GNSS in case of loss of availability, and provides an additional integrity check. However, it only propagates the previous GNSS ACC95/PL. Therefore, performance compliance must be evaluated with both M(G)RAIM algorithms.

For navigation phases where VAIM performance is not sufficient, different GNSS solutions should be explored until the accuracy and protection level (PL) are within the expected range. Then, better dead reckoning sensors could improve the stability and availability of the navigation solution.

However, VAIM requires safe characterization of dead reckoning errors. INSPIRe has considered an error model to generate synthetic data, but the safety of the concept in a real application depends on the characterization of the error. This will be a key technical activity for operational VAIM development.

Regarding operational considerations, VAIM implementation in SOLAS vessels should be easy and quick. There are no regulatory barriers. In fact, VAIM is aligned with the aforementioned IMO regulations [RD.3] and [RD.4] and could already be implemented for the dead reckoning sensors that are already mandatory. The only complexity could be the implementation of a centralized element where information from GNSS and dead reckoning sensors is provided and fused.

The cost of implementation is limited to the new central element if it does not already exist on the vessel. Otherwise, the cost is negligible since the sensors used in VAIM are already mandatory and do not require additional processing capabilities. Every element is already on board, and only the vessel's software would require an upgrade. Vessels already have sensors that allow them to navigate in each phase, so it is not expected that any additional sensors or costs will be required.

However, the penetration of this technology typically takes a long time, as mariners only change their equipment when required to do so or when they see a clear advantage. The need for integrity in maritime is still under question, so a slow rate of navigation equipment upgrade is expected.

End of Document